PARAMETRIC OPTIMIZATION OF FUSED DEPOSITION MODELING USING RESPONSE SURFACE METHODOLOGY

A THESIS SUBMITTED IN PARTIAL FULFILLMENT

FOR THE REQUIREMENT FOR THE DEGREE OF

Master of Technology

in

Production Engineering

by

VEDANSH CHATURVEDI

Department of Mechanical Engineering

National Institute of Technology

Rourkela – 8

2009

PARAMETRIC OPTIMIZATION OF FUSED DEPOSITION MODELING USING RESPONSE SURFACE METHODOLOGY

A THESIS SUBMITTED IN PARTIAL FULFILLMENT

FOR THE REQUIREMENT FOR THE DEGREE OF

Master of Technology

in

Production Engineering

by

VEDANSH CHATURVEDI

Under the guidance of

Dr. S. S. MAHAPATRA

Professor, Department of Mechanical Engineering

Department of Mechanical Engineering

National Institute of Technology

Rourkela – 8

2009

National Institute of Technology

Rourkela

CERTIFICATE

This is to certify that the thesis entitled, "PARAMETRIC OPTIMIZATION OF FUSED MODELING USING RESPONSE SURFACE METHODOLOGY" submitted by Vedansh Chaturvedi in partial fulfillment of the requirements for the award of Master of Technology Degree in Mechanical Engineering with specialization in Production Engineering at the National Institute of Technology, Rourkela (deemed University) is an authentic work carried out by him under my supervision and guidance.

To the best of my knowledge, the matter embodied in the thesis has not submitted to any other University/Institute for the award of any degree or diploma.

Dr. S. S. Mahapatra

Date:

Dept. of Mechanical Engineering
National Institute of Technology
Rourkela – 769008

ACKNOWLEDGEMENT

I would like to express my deep sense of respect and gratitude toward my supervisor **Dr. S. S. Mahapatra**, who not only guided the academic project work but also stood as a teacher and philosopher in realizing the imagination in pragmatic way, I want to thank him for introducing me for the field of Optimization and giving the opportunity to work under him. His presence and optimism have provided an invaluable influence on my career and outlook for the future. I consider it my good fortune to have got an opportunity to work with such a wonderful person.

I express my gratitude to **Dr. R. K. Sahoo**, Professor and Head, Department of Mechanical Engineering, faculty member and staff of Department of Mechanical Engineering for extending all possible help in carrying out the dissertation work directly or indirectly. They have been great source of inspiration to me and I thank them from bottom of my heart. I like to express my gratitude to **Dr**. **Saurav Datta,** Lecturer, Department of Mechanical Engineering , for his valuable advice in carrying out Literature review.

I am especially indebted to my parents for their love, sacrifices and support. They are my teachers after I came to this world and have set great example for me about how to live, study and work.

VEDANSH CHATURVEDI

CONTENTS

ABSTRACT

Fused deposition modeling (FDM) is a process for developing rapid prototype (RP) objects by depositing fused layers of material according to numerically defined cross sectional geometry. The quality of FDM produced parts is significantly affected by various parameters used in the process. This dissertation work aims to study the effect of five process parameters such as layer thickness, sample orientation, raster angle, raster width, and air gap on mechanical property of FDM processed parts. In order to reduce experimental runs, response surface methodology (RSM) based on central composite design is adopted. Specimens are prepared for tensile, flexural, and impact test as per ASTM standards. Empirical relations among responses and process parameters are determined and their validity is proved using analysis of variance (ANOVA) and the normal probability plot of residuals. Response surface plots are analyzed to establish main factor effects and their interaction on responses. Optimal factor settings for maximization of each response have been determined. Major reason for weak strength of FDM processed parts may be attributed to distortion within the layer or between the layers while building the parts due to temperature gradient. Since RP parts are subjected to different loading conditions, practical implication suggests that more than one response must be optimized simultaneously. To this end, mechanical properties like tensile strength, bending strength, and impact strength of the produced component are considered as multiple responses and simultaneous optimization has been carried out with the help of response optimizer. Grey relation has been employed to convert multiple responses into a single response for optimization purpose. It is interesting to note that factor level settings for simultaneous optimization of all responses significantly differ from optimization with single response.

LIST OF FIGURES

LIST OF TABLES

NOMENCLATURE

RP	Rapid prototyping
STL	Stereolithography
FDM	Fused deposition modeling
ABS	Acrylonitrile butadiene styrene
RSM	Response surface methodology
CCD	Central composite design
ANOVA	Analysis of variance
SS	Sum of square
MS	Mean sum of square
DF	Degree of freedom
SEM	Scanning electron microscope
GRA	Grey relational analysis
GRG	Grey relational grade

CHAPTER 1

AN INTRODUCTION TO RAPID PROTOTYPING

1. Introduction

1.1 Overview of Rapid Prototyping:

The term rapid prototyping (RP) refers to a class of technologies that can automatically construct physical models from Computer-Aided Design (CAD) data. These "three dimensional printers" allow designers to quickly create tangible prototypes of their designs, rather than just two-dimensional pictures. Such models have numerous uses. They make excellent visual aids for communicating ideas with co-workers or customers. In addition, prototypes can be used for design testing. For example, an aerospace engineer might mount a model airfoil in a wind tunnel to measure lift and drag forces. Designers have always utilized prototypes; RP allows them to be made faster and less expensively.

In addition to prototypes, RP techniques can also be used to make tooling (referred to as *rapid tooling*) and even production-quality parts (rapid manufacturing). For small production runs and complicated objects, rapid prototyping is often the best manufacturing process available. Of course, "rapid" is a relative term. Most prototypes require from three to seventy-two hours to build, depending on the size and complexity of the object. This may seem slow, but it is much faster than the weeks or months required to make a prototype by traditional means such as machining. These dramatic time savings allow manufacturers to bring products to market faster and more cheaply. In 1994, Pratt & Whitney achieved "an order of magnitude [cost] reduction [and] . . . time savings of 70 to 90 percent" by incorporating rapid prototyping into their investment casting process.

At least six different rapid prototyping techniques are commercially available, each with unique strengths. Because RP technologies are being increasingly used in non-prototyping applications,

the techniques are often collectively referred to as solid free-form fabrication; computer automated manufacturing, or layered manufacturing. The latter term is particularly descriptive of the manufacturing process used by all commercial techniques. A software package "slices" the CAD model into a number of thin (~0.1 mm) layers, which are then built up one atop another. Rapid prototyping is an "additive" process, combining layers of paper, wax, or plastic to create a solid object. In contrast, most machining processes (milling, drilling, grinding, etc.) are "subtractive" processes that remove material from a solid block. RP's additive nature allows it to create objects with complicated internal features that cannot be manufactured by other means.

Of course, rapid prototyping is not perfect. Part volume is generally limited to 0.125 cubic meters or less, depending on the RP machine. Metal prototypes are difficult to make, though this should change in the near future. For metal parts, large production runs, or simple objects, conventional manufacturing techniques are usually more economical. These limitations aside, rapid prototyping is a remarkable technology that is revolutionizing the manufacturing process.

1.2 The Basic Process

Although several rapid prototyping techniques exist, all employ the same basic five-step process. The steps are:

1. Create a CAD model of the design
2. Convert the CAD model to STL format
3. Slice the STL file into thin cross-sectional layers
4. Construct the model one layer atop another
5. Clean and finish the model

CAD Model Creation: First, the object to be built is modeled using a Computer-Aided Design (CAD) software package. Solid modelers, such as Pro/ENGINEER, tend to represent 3-D objects more accurately than wire-frame modelers such as AutoCAD, and will therefore yield better results. The designer can use a pre-existing CAD file or may wish to create one expressly for prototyping purposes. This process is identical for all of the RP build techniques.

Conversion to STL Format: The various CAD packages use a number of different algorithms to represent solid objects. To establish consistency, the STL (stereolithography), the first RP technique) format has been adopted as the standard of the rapid prototyping industry. The second step, therefore, is to convert the CAD file into STL format. This format represents a three-dimensional surface as an assembly of planar triangles, "like the facets of a cut jewel." The file contains the coordinates of the vertices and the direction of the outward normal of each triangle. Because STL files use planar elements, they cannot represent curved surfaces exactly. Increasing the number of triangles improves the approximation, but at the cost of bigger file size. Large, complicated files require more time to pre-process and build, so the designer must balance accuracy with manageability to produce a useful STL file. Since the .stl format is universal, this process is identical for all of the RP build techniques.

Slice the STL File: In the third step, a pre-processing program prepares the STL file to be built. Several programs are available, and most allow the user to adjust the size, location and orientation of the model. Build orientation is important for several reasons. First, properties of rapid prototypes vary from one coordinate direction to another. For example, prototypes are usually weaker and less accurate in the z (vertical) direction than in the x-y plane. In addition, part orientation partially determines the amount of time required to build the model. Placing the shortest dimension in the z direction reduces the number of layers, thereby shortening build time.

The pre-processing software slices the STL model into a number of layers from 0.01 mm to 0.7 mm thick, depending on the build technique. The program may also generate an auxiliary structure to support the model during the build. Supports are useful for delicate features such as overhangs, internal cavities, and thin-walled sections. Each PR machine manufacturer supplies their own proprietary pre-processing software.

Layer by Layer Construction: The fourth step is the actual construction of the part. Using one of several techniques (described in the next section) RP machines build one layer at a time from polymers, paper, or powdered metal. Most machines are fairly autonomous, needing little human intervention.

Clean and Finish: The final step is post-processing. This involves removing the prototype from the machine and detaching any supports. Some photosensitive materials need to be fully cured before use. Prototypes may also require minor cleaning and surface treatment. Sanding, sealing, and/or painting the model will improve its appearance and durability.

1.3 Rapid Prototyping Techniques

Most commercially available rapid prototyping machines use one of six techniques. At present, trade restrictions severely limit the import/export of rapid prototyping machines, so this guide only covers systems available in the U.S.

1.3.1 Stereolithography:

Stereolithography is an additive fabrication process utilizing a vat of liquid UV-curable photopolymer "resin" and a UV laser to build parts a layer at a time. On each layer, the laser beam traces a part cross-section pattern on the surface of the liquid resin. Exposure to the UV laser light cures, or, solidifies the pattern traced on the resin and adheres it to the layer below.

After a pattern has been traced, the SLA's elevator platform descends by a single layer thickness, typically 0.05 mm to 0.15 mm (0.002" to 0.006"). Then, a resin-filled blade sweeps across the part cross section, re-coating it with fresh material. On this new liquid surface the subsequent layer pattern is traced, adhering to the previous layer. A complete 3-D part is formed by this process. After building, parts are cleaned of excess resin by immersion in a chemical bath and then cured in a UV oven.

Stereolithography requires the use of support structures to attach the part to the elevator platform and to prevent certain geometry from not only deflecting due to gravity, but to also accurately hold the 2-D cross sections in place such that they resist lateral pressure from the re-coater blade. Supports are generated automatically during the preparation of 3-D CAD models for use on the stereolithography machine, although they may be manipulated manually. Supports must be removed from the finished product manually; this is not true for all rapid prototyping technologies.

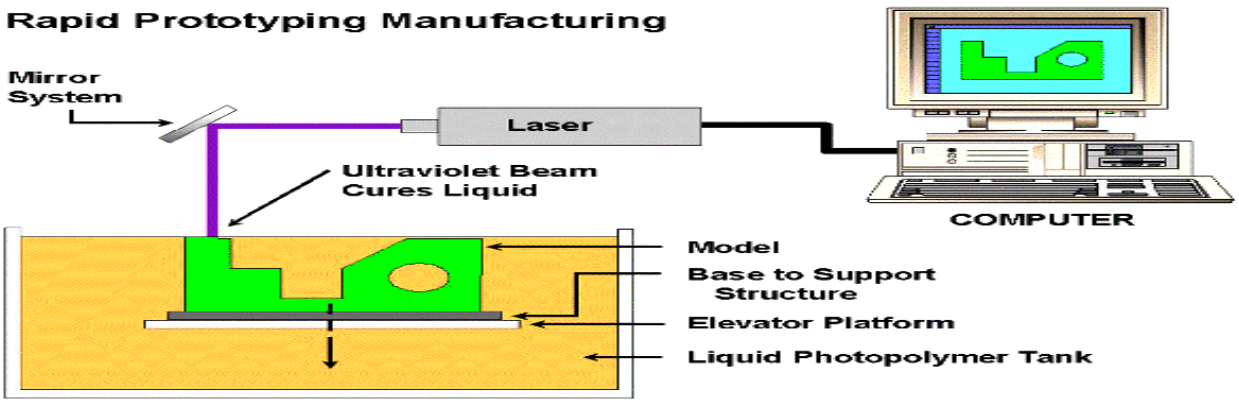

Figure 1.1 Stereolithography

Application Range

- Parts used for functional tests.

- Manufacturing of medical models.
- Form –fit functions for assembly tests.

Advantages

- Possibility of manufacturing parts which are impossible to be produced conventionally in a single process.
- Can be fully atomized and no supervision is required.
- High Resolution.

Disadvantages

- Necessity to have a support structure.
- Require labor for post processing and cleaning.

1.3.2 Selective Laser Sintering:

Selective laser sintering is an additive rapid manufacturing technique that uses a high power laser (for example, a carbon dioxide laser) to fuse small particles of plastic, metal, ceramic, or glass powders into a mass representing a desired 3-dimensional object. The laser selectively fuses powdered material by scanning cross-sections generated from a 3-D digital description of the part (for example from a CAD file or scan data) on the surface of a powder bed. After each cross-section is scanned, the powder bed is lowered by one layer thickness, a new layer of material is applied on top, and the process is repeated until the part is completed.Compared to other rapid manufacturing methods, SLS can produce parts from a relatively wide range of commercially available powder materials, including polymers (nylon, also glass-filled or with other fillers, and polystyrene), metals (steel, titanium, alloy mixtures, and composites) and green sand. The physical process can be full melting, partial melting, or liquid-phase sintering. And,

depending on the material, up to 100% density can be achieved with material properties comparable to those from conventional manufacturing methods. In many cases large numbers of parts can be packed within the powder bed, allowing very high productivity.SLS is performed by machines called SLS systems; the most widely known model of which is the Sinterstation SLS system. SLS technology is in wide use around the world due to its ability to easily make very complex geometries directly from digital CAD data. While it began as a way to build prototype parts early in the design cycle, it is increasingly being used in limited-run manufacturing to produce end-use parts. One less expected and rapidly growing application of SLS is its use in art. SLS was developed and patented by Dr. Carl Deckard at the University of Texas at Austin in the mid-1980s, under sponsorship of DARPA. A similar process was patented without being commercialized by R.F. Housholder in 1979.Unlike some other Rapid Prototyping processes, such as Stereolithography (SLA) and Fused Deposition Modeling (FDM), SLS does not require support structures due to the fact that the part being constructed is surrounded by unsintered powder at all times.

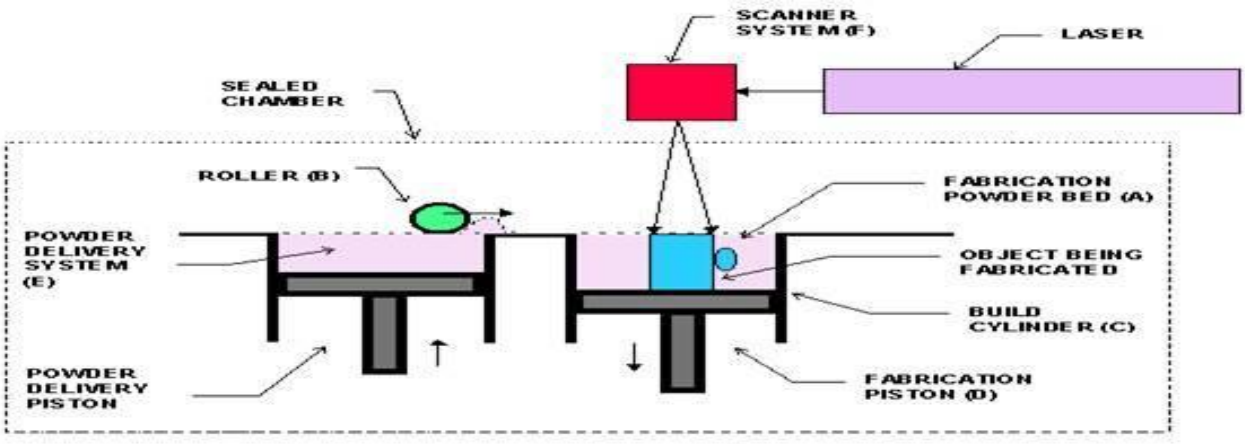

Figure 1.2 Selective laser sintering

Application Range

- Visual Representation models.
- Functional and tough prototypes.
- cast metal parts.

Advantages

- Flexibility of materials used.
- No need to create a structure to support the part.
- Parts do not require any post curing except when ceramic is used.

Disadvantages

- During solidification, additional powder may be hardened at the border line.
- The roughness is most visible when parts contain sloping (stepped) surfaces.

1.3.3 Laminated object manufacturing:

Profiles of object cross sections are cut from paper or other web material using a laser. The paper is unwound from a feed roll onto the stack and first bonded to the previous layer using a heated roller which melts a plastic coating on the bottom side of the paper. The profiles are then traced by an optics system that is mounted to an X-Y stage. After cutting of the layer is complete, excess paper is cut away to separate the layer from the web. Waste paper is wound on a take-up roll. The method is self-supporting for overhangs and undercuts. Areas of cross sections which are to be removed in the final object are heavily cross-hatched with the laser to facilitate removal. It can be time consuming to remove extra material for some geometry, however. In general, the finish, accuracy and stability of paper objects are not as good as for materials used with other RP methods. However, material costs are very low, and objects have the look and feel

of wood and can be worked and finished in the same manner. This has fostered applications such as patterns for sand castings. While there are limitations on materials, work has been done with plastics, composites, ceramics and metals. Some of these materials are available on a limited commercial basis. Variations on this method have been developed by many companies and research groups. For example, Kira's Paper Lamination Technology (PLT) uses a knife to cut each layer instead of a laser and applies adhesive to bond layers using the xerographic process. Solido Ltd. of Israel (formerly Solidimension) also uses a knife, but instead bonds layers of plastic film with a solvent. There are also variations which seek to increase speed and/or material versatility by cutting the edges of thick layers diagonally to avoid stair stepping. The principal US commercial provider of laser-based LOM systems, Helisys, ceased operation in 2000. However the company's products are still sold and serviced by a successor organization, Cubic Technologies.

The process is performed as follows:

1. Sheet is adhered to a substrate with a heated roller.
2. Laser traces desired dimensions of prototype.
3. Laser cross hatches non-part area to facilitate waste removal.
4. Platform with completed layer moves down out of the way.
5. Fresh sheet of material is rolled into position.
6. Platform moves up into position to receive next layer.
7. The process is repeated.

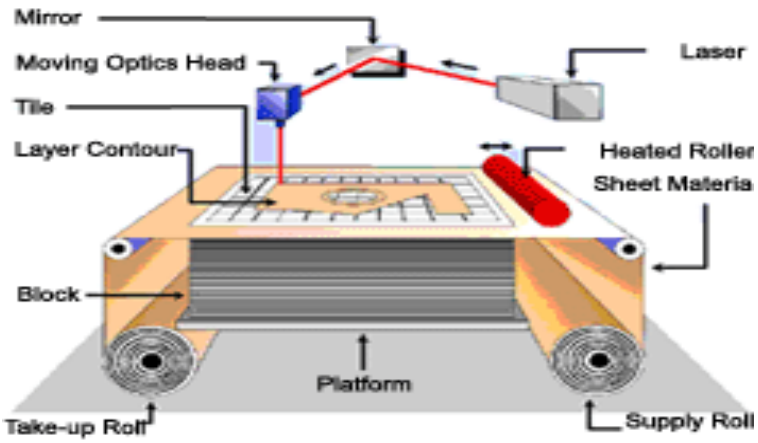

Figure 1.3 Laminated object manufacturing

Application Range

- Visual Representation models
- Large Bulky models as sand casting patterns

Advantages

- Variety of organic and inorganic materials such as paper, plastic, ceramic, composite can be used
- Process is faster than other processes
- No internal stress and undesirable deformations
- LOM can deal with discontinuities, where objects are not closed completely

Disadvantages

- The stability of the object is bonded by the strength of the glued layers.
- Parts with thin walls in the z direction can not be made using LOM
- Hollow parts can not be built using LOM

1.3.4 Fused Deposition Modeling

Fused deposition modeling, which is often referred to by its initials FDM, is a type of additive fabrication or (sometimes called rapid prototyping/rapid manufacturing (RP or RM)) technology commonly used within engineering design[1]. The technology was developed by S. Scott Crump in the late 1980s and was commercialized in 1990. The FDM technology is marketed commercially by Stratasys, which also holds a trademark on the term.

Like most other additive fabrication processes (such as 3D printing and stereolithography) FDM works on an "additive" principle by laying down material in layers. A plastic filament or metal wire is unwound from a coil and supplies material to an extrusion nozzle which can turn on and off the flow. The nozzle is heated to melt the material and can be moved in both horizontal and vertical directions by a numerically controlled mechanism, directly controlled by a computer-aided manufacturing (CAM) software package [2]. The model or part is produced by extruding small beads of thermoplastic material to form layers as the material hardens immediately after extrusion from the nozzle.

Several materials are available with different trade-offs between strength and temperature properties. As well as acrylonitrile butadiene styrene (ABS) polymer, the FDM technology can also be used with polycarbonates, polycaprolactone, polyphenylsulfones and waxes. A "water-soluble" material can be used for making temporary supports while manufacturing is in progress[3]. Marketed under the name Waterworks by Stratasys, this soluble support material is quickly dissolved with specialized mechanical agitation equipment utilizing a precisely heated sodium hydroxide solution.

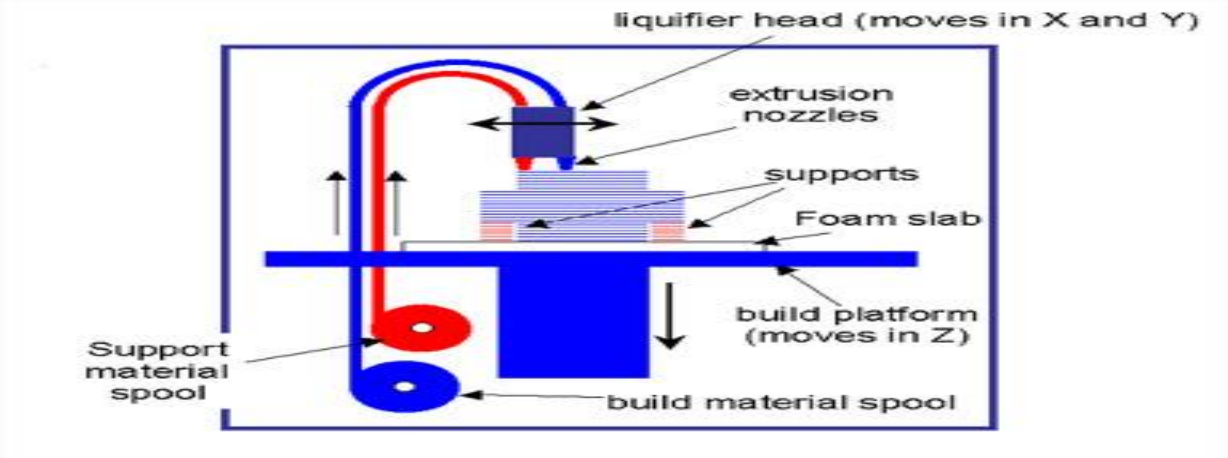

Figure 1. 4 Fused deposition modeling

Application Range

- Conceptual modeling
- Fit, form applications and models for further manufacturing procedures
- Investment casting and injection molding

Advantages

- Quick and cheap generation of models
- There is no worry of exposure to toxic chemicals, lasers or a liquid chemical bath.

Disadvantages

- Restricted accuracy due to the shape of material used, wire is 1.27 mm diameter.

1.4 Objective of Research Work

The competition in world market for manufactured product has intensified tremendously in recent years. It has become important for new products to reach the market as early as possible. As a result reduction of product development cycle time is a major concern in industries for achieving competitive advantage. Now days the focus of industries has shifted from traditional product development methodology to accelerated or rapid fabrication techniques. Some of the

latest developments within the automotive industry have shown how emerging rapid prototyping and manufacturing (RP&M) technologies can be used to reduce lead time in the prototype development process. The main benefit rapid prototyping (RP) technologies offer as compared to conventional subtractive and formative manufacturing process is that virtually any complex geometry can be built in a layer wise manner directly from CAD model of part without the need for tooling using a nearly fully automated process. This ability to fabricate complex geometry at no extra cost is virtually unheard in traditional manufacturing, where there is direct link between cost of component and complexity of design. On the other hand absence of tooling means that manufacturing inputs are not required in order to design parts and products . For example if RP is used to manufactured the part which was conventionally manufactured by injection moulding, considerations for draft angles, ejection pins and gates marks, wall thickness, sharp corners, weld lines and parting lines is not important for part design. This directly means whatever can be designed it can be manufactured. That is optimal design can be selected for manufacturing without considering the feasibility of their production in terms of available manufacturing technology. Incorporating features such as undercuts, blind holes, screws in process like injection moulding often requires expensive tooling, extensive tool setups and testing runs and inevitably leads to undesirable lead times and costs. Also there is a threshold limit for minimum production level which has to be cross to offset the cost of tooling. This result in high volume manufacturing to compensate the tooling cost. Whereas the possibility of producing highly complex, cost effective custom parts is apparent in RP . Another noted advantage of RP is their ability to produce functional assembly by consolidating sub assemblies into single unit at the computer aided design (CAD) stage thus reducing the part count, handling time storage requirement and without considering the mating and fit problem. RP allows the deposition of

multiple materials in any location or combination that the designer requires. This has potentially enormous implications for the functionality and aesthetics that can be designed into parts .

Having such enormous advantages one of the biggest hindrance in the full scale application of RP technologies is available materials and their properties, which substantially differ from the properties of generally used materials. To overcome this limitation one approach is to develop new materials which can be used by RP machines and have properties superior or as par with conventional materials. Another procedure is to suitably adjust the process parameters for RP part fabrication for maximum improvement in the properties. Number of researchers contributed in this second approach. Their works reveal that properties of RP parts are function of various process related parameters and can be significantly improved with their proper adjustment. Since mechanical strength is an important requirement for the functional part there is great need to improve them. With this aim in mind the present study focus on the mechanical properties viz. tensile, flexural and impact strength of part fabricated using fused deposition modeling (FDM) technology and derive the quantitative relation between the processing parameters and mechanical strength so that the mechanical response of the processed part must be predictable over the allowable range of parameter.

CHAPTER 2

A BRIEF LITERATURE REVIEW

2. Literature review

Ahn et al. [4] Uses design of experiment method and concluded that the air gap and raster orientation affect the tensile strength of FDM processes part where as raster width, model temperature and colour have little effect. They further compare the measured tensile strength of FDM part processed at different raster angles and air gap with the tensile strength of injection moulded part. Material use for both type of fabrication is ABSP400. With zero air gap FDM specimen tensile strength lies between 10%-73% of injection moulded part with maximum at 0° and minimum at 90° raster orientation with respect to loading direction. But with negative air gap there is significant increase in strength at respective raster orientation but still it is less than the injection moulded part. All specimens failed in transverse direction except for specimen whose alternate layer raster angle varies between 45° and -45°. This type of specimen failed along the 45° line. Compression test on the specimen build at two different orientations revealed that this strength is higher than the tensile strength and lies between 80 to 90% of those for injection moulded part. Also specimen build with axis perpendicular to build table shows less compressive strength as compared to specimen build with axis parallel to build table. Based on these observations it was concluded that strength of FDM processed part is anisotropic.

Es Said et al. [5] Study the effect of raster angle on the tensile, bending and impact properties of FDM ABSP400 part made using FDM1650 machine. There observations indicate that raster orientation effect the strength as polymer molecules align themselves along the direction of flow. Also FDM follows phase change for constructing solid model from solid filament extruded from nozzle tip in semi molten state and solidify in a chamber maintain at particular temperature. As a

result volumetric shrinkage takes place which results in weak interlayer bonding and cause porosity which reduce the load bearing area.

Lee et al. [6] Performed experiments on cylindrical parts made using three RP processes FDM, 3D printer and nano composite deposition (NCDS) to study the effect of build direction on the compressive properties. Experimental results show that compressive strength is 11.6% higher for axial FDM specimen as compared to transverse FDM specimen. In 3D printing, diagonal specimen possesses maximum compressive strength in comparison to axial specimen. For NCDS, axial specimen showed compressive strength 23.6% higher than that of transverse specimen. Out of three RP technologies, parts built by NCDS are most affected by the build direction.

Khan et al. [7] concluded that layer thickness, raster angle and air gap are found to be significantly affect the elastic performance of the compliant FDM ABS prototype.

Wang et al. [8], in their work, has mentioned that as extruded material from nozzle cools from its glass transition temperature to chamber temperature inner stresses will develop particularly due to uneven deposition speed. These inner stresses will cause the inter layer and the intra layer deformation which will result in cracking, de-lamination or even part fabrication failure. Thus affect the part strength and size. They propose the mathematical model to study the effect of total number of layers, stacking section length, and chamber temperature on the above mentioned deformations. They concluded that as the total number of layers increase deformation will decrease rapidly but decreasing tendency will become slow after certain number of layers, higher stacking section lengths will produce large deformations and as chamber temperature will increase deformation will decrease and become zero at the glass transition temperature of

material. Based on these results they propose that material use for part fabrication must have lower glass transition temperature and linear shrinkage rate. Also the extruded fiber length must be small.

Bellehumeur et al. [9] experimentally assessed the bond quality between adjacent filaments and their failure under flexural loading. Experimental results showed that both the envelope temperature and variations in the convective conditions with in the building chamber have strong effect on the meso-structure and the overall quality of bond strength. On line measurements of the cooling temperature profiles reveals that temperature profile of bottom layers rises above the glass transition temperature followed by rapid decrease as the extrusion head moves away from the position of placement of thermoset and minimum temperature increase with the number of layers. Microphotograph of the cross sectional area shows diffusion of adjacent filaments is more in lower layers as compared to upper layers for the face of specimen with higher number of layers.

Chou and Zang [10], in their work, simulated the FDM process using finite element analysis (FEA) and analyzes the effect of tool path patterns on residual stresses and part distortions. At each layer stress starts to accumulate at the locations of initial deposition and at tool path turning point. During the deposition process, the residual stress is smallest for most recently activated elements as compare to earlier activated element. The residual effect on the bottom surface of each layer corresponds to stress concentration pattern of its bottom layer. For the long raster pattern stress concentration characteristic is aligned along the length side and along the width side for the short raster deposition. Thus the maximum stress zone shifts from the center of the part towards the length side and width side for the long and short raster pattern respectively. Simulated results are found to be in agreement with experimental results of the distortion in part

except the magnitude of distortion is more than the expected and this may be due to simplified material properties and boundary conditions assumed during simulation.

Above mention work reveals that the mechanical properties of FDM processed part exhibit anisotropy and are sensitive to the processing parameters that affect the meso-structure and fibre-to-fibre bond strength. Also un-even heating and cooling cycles due to inherent nature of FDM build methodology results in stress accumulation in the build part and these stress concentration regions will also affect the strength. It is also observed that all the researches in FDM strength modeling is basically devoted to study the effect of processing conditions on the part strength with no significant effort made to develop the strength model in terms of FDM process parameters so as to predict in advance the strength of component for practical application.

Anitha et al. [11]**, i**n their result, revealed several interesting features of the FDM process Only the layer thickness is effective to 49.37% at 95% level of significance. But on pooling, it was found that the layer thickness is effective to 51.57% at 99% level of significance. The other factors, road width and speed , contributes to 15.57 and 15.83% at 99% level of significance, respectively. The significance of layer thickness is further strengthened by the correlation analysis. Which indicates a strong inverse relationship with surface roughness.

According to the S/N analysis, the layer thickness is most effective when it is at level 3(0.3556mm), the road width at level 1(0.537mm) and the speed of deposition at level 3 (200mm).According to this trials , sample 18 was found to give the best results.

Agrawal et al. [12] In this work, the concept of stochastic modelling of tolerances and clearances has been extended to RP processes. Using the unified approach for RP processes, the mechanical error in the FD process has been studied. A methodology has been developed to analyse the mechanical error at the nozzle tip of the FD process for input values of the tolerances

and clearances, where the links and hinges are produced on a mass scale. Closed-form expressions have been derived to find the mechanical error in the coordinates of a point on the work surface. It is observed that the influence coefficients of the z coordinate of a point on the work surface have a larger magnitude than those of the x and y coordinates. The three-sigma bands obtained in tracing a few example curves by the nozzle tip are plotted. The variances and their sum are listed in a table to show their variation across the work surface.

The overall error is found to vary appreciably across the work surface. The error is minimum at the front-left end of the work surface and maximum at the rear-right end. The methodology can be extended for the optimal allocation of tolerances and clearances to reduce the cost of manufacturing.

Pandey et al. [13] In this research they found Orientation for part deposition is one of the important factors as it affects average part surface roughness and production time. In the present work, two objective functions, namely average part surface roughness and build time, are formulated.

NSGA-II is successfully used to determine a set of pareto optimal solutions for part deposition orientation for the two contradicting objectives. It can be seen from the results obtained for different parts that there exist two limiting situations. One is minimum average part surface roughness with maximum production time and another is minimum production time with maximum average part surface roughness. The developed system of part deposition orientation determination also gives a set of intermediate solutions in which any solution can be used depending upon the pre- ference of user for the two objectives. The present system can be used for any class of component, which may be a freeform or a regular object.

CHAPTER 3

FUSED DEPOSITION MODELLING AND ABS MATERIAL

3. Fused deposition modeling and ABS material

3.1 Fused Deposition Modeling

FDM is one of the RP technology developed by Stratasys, USA (Figure 3.1). But unlike other RP systems which involve an array of lasers, powders, resins, this process uses heated thermoplastic filaments which are extruded from the tip of nozzle in a temperature controlled environment. For this there is a material deposition subsystem known as head (Figure 3.2) which consist of two liquefier tips. One tip for model material and other tip for support material deposition both of which works alternatively. The article forming material is supplied to the head in the form of a flexible strand of solid material from a supply source (reel). One pair of pulleys or rollers having a nip in between are utilized as material advance mechanism to grip a flexible strand of modeling material and advance it into a heated dispensing or liquefier head. The material is heated above its solidification temperature by a heater on the dispensing head and extruded in a semi molten state on a previously deposited material onto the build platform following the designed tool path. The head is attached to the carriage that moves along the X-Y plane. The build platform moves along the Z direction. The drive motion are provided to selectively move the build platform and dispensing head relative to each other in a predetermined pattern through drive signals input to the drive motors from CAD/CAM system. The fabricated part takes the form of a laminate composite with vertically stacked layers, each of which consists of contiguous material fibres or rasters with interstitial voids. Fibre-to-fibre bonding within and between layers occurs by a thermally-driven diffusion bonding process during solidification of the semi-liquid extruded fibre [14].

FDM Vantage uses insight software to import STL file automatically slice the file, generate necessary support structure and material extrusion path [15].

Power required - 230 V,AC

Motor - 50/60 Hz,3Φ

Max. room temperature - 29.3^{o}C

Size of the system - 1277mm wide X 874 mm deep X 1950 mm hight

Figure 3.1 FDM Vantage machine SE

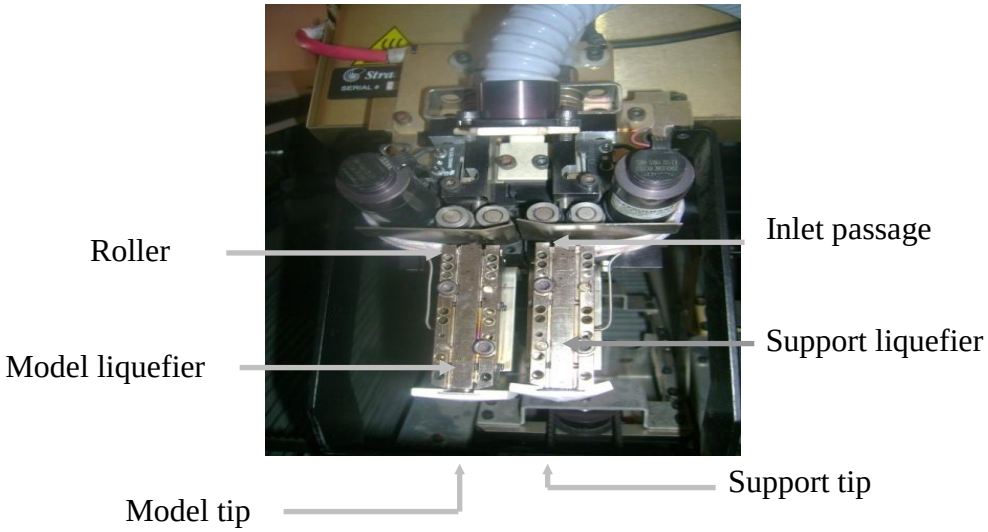

Figure 3.2 Head Assembly of FDM Vantage SE

Main process parameters involved in part fabrication are [3.3]:

1. **Orientation**: Part builds orientation or orientation referrers to the inclination of part in a build platform with respect to X, Y, Z axis. Where X and Y-axis are considered parallel to build platform and Z-axis is along the direction of part build.
2. **Layer thickness:** It is a thickness of layer deposited by nozzle and depends upon the type of nozzle used.
3. **Part Fill Style:** Determines the manner in which nozzle will deposit the material in a single layer of a part. There are two types of part fill methods:

   Perimeter Raster: Outer boundary is contour (perimeter) and internal is filled with raster.

   Contours to depth: Other then the outer contour additional contours are provided to fill the inner region and remaining inner region is filled with raster. The number of additional contours is determined by the depth of contours value. By default depth of contour is twice the contour width to produce one contour.
4. **Contour width:** The width of contour deposited by nozzle.
5. **Part raster width** (raster width)**:** Width of raster pattern used to fill interior regions of part curves.
6. **Part interior style:** Determine how the interior area in each layer is filled. There are two methods:

   Solid normal: Fills the part completely

   Sparse: Semi hollow interior (honeycomb structure), minimize the amount of material used.
7. **Visible surface**: This feature improves the part external appearance.
8. **Raster angle**: It is a direction of raster relative to the x-axis of build table.

9. **Shrinkage factor**: Shrinkage factor applied in the x, y and z direction.
10. **Perimeter to raster air gap**: The gap between inner most contours and the edge of the raster fill inside of the contour.
11. **Raster to raster gap** (air gap): It is the gap between two adjacent rasters on same layer.

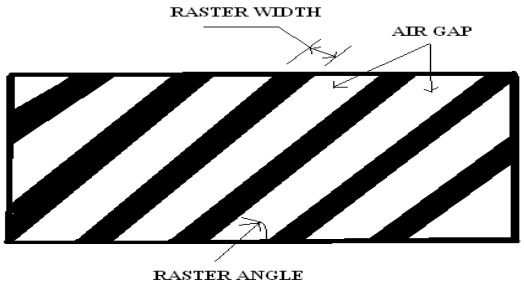

Figure 3.3 showing process parameter of FDM

3.2 ABS (Acrylonitrile butadiene styrene) material:

Acrylonitrile Butadiene Styrene (**ABS**) chemical formula $(C_8H_8 \cdot C_4H_6 \cdot C_3H_3N)_n$) is a common thermoplastic used to make light, rigid, molded products such as piping (for example Plastic Pressure Pipe Systems), musical instruments (most notably recorders and plastic clarinets), golf club heads (used for its good shock absorbance), automotive body parts, wheel covers, enclosures, protective head gear, buffer edging for furniture and joinery panels, airsoft BBs and toys, including Lego bricks. ABS plastic ground down to an average diameter of less than 1 micrometer is used as the colorant in some tattoo inks. Tattoo inks that use ABS are extremely vivid. This vividness is the most obvious indicator that the ink contains ABS, as tattoo inks rarely list their ingredients [4] .

It is a copolymer made by polymerizing styrene and acrylonitrile in the presence of polybutadiene. The proportions can vary from 15 to 35% acrylonitrile, 5 to 30% butadiene and

40 to 60% styrene. The result is a long chain of polybutadiene criss-crossed with shorter chains of poly(styrene-co-acrylonitrile). The nitrile groups from neighboring chains, being polar, attract each other and bind the chains together, making ABS stronger than pure polystyrene. The styrene gives the plastic a shiny, impervious surface. The butadiene, a rubbery substance, provides resilience even at low temperatures. ABS can be used between −25 and 60 °C. The properties are created by rubber toughening, where fine particles of elastomer are distributed throughout the rigid matrix.

Production of 1 kg of ABS requires the equivalent of about 2 kg of oil for raw materials and energy. It can also be recycling.

3.3 Properties of ABS plastic

ABS is derived from acrylonitrile, butadiene, and styrene. Acrylonitrile is a synthetic monomer produced from propylene and ammonia; butadiene is a petroleum hydrocarbon obtained from the C4 fraction of steam cracking; styrene monomer is made by dehydrogenation of ethyl benzene - a hydrocarbon obtained in the reaction of ethylene and benzene. The advantage of ABS is that this material combines the strength and rigidity of the acrylonitrile and styrene polymers with the toughness of the polybutadiene rubber. The most important mechanical properties of ABS are resistance and toughness. A variety of modifications can be made to improve impact resistance, toughness, and heat resistance. The impact resistance can be amplified by increasing the proportions of polybutadiene in relation to styrene and also acrylonitrile although this causes changes in other properties. Impact resistance does not fall off rapidly at lower temperatures. Stability under load is excellent with limited loads [7].

Even though ABS plastics are used largely for mechanical purposes, they also have good electrical properties that are fairly constant over a wide range of frequencies. These properties

are little affected by temperature and atmospheric humidity in the acceptable operating range of temperatures. The final properties will be influenced to some extent by the conditions under which the material is processed to the final product; for example, molding at a high temperature improves the gloss and heat resistance of the product whereas the highest impact resistance and strength are obtained by molding at low temperature.

ABS polymers are resistant to aqueous acids, alkalis, concentrated hydrochloric and phosphoric acids, alcohols and animal, vegetable and mineral oils, but they are swollen by glacial acetic acid, carbon tetrachloride and aromatic hydrocarbons and are attacked by concentrated sulfuric and nitric acids. They are soluble in esters, ketones and ethylene dichloride.

The aging characteristics of the polymers are largely influenced by the polybutadiene content, and it is normal to include antioxidants in the composition. On the other hand, while the cost of producing ABS is roughly twice the cost of producing polystyrene, ABS is considered superior for its hardness, gloss, toughness, and electrical insulation properties. However, it will be degraded (dissolve) when exposed to acetone. ABS is flammable when it is exposed to high temperatures, such as a wood fire. It will "boil", then burst spectacularly into intense, hot flames.

Table 3.1 ABS material data sheet

Properties	Specifications
Structure	Amorphous
Specific density	1.05
Water absorption rate (%)	0.27
Elongation (%)	20
Tensile strength (MPa)	29.64
Compression strength (MPa)	62.05
Flexural strength (MPa)	63.43
Flexural modulus (MPa)	2068.48
Impact (joules)	8.94
Hardness	R110
Ultrasonic welding	Excellent

Bonding	Excellent
Machining	Good
Min. utilization temperature (deg. C)	-40
Max. utilization temperature (deg .C)	90
Melting point (deg.C)	105
Coefficient of expansion	0.000053
Arc resistance	80
Dielectric strength (KV/mm)	16
Transparency	Translucent
UV Resistance	Poor
Chemical resistance	Good

CHAPTER 4

RESPONSE SURFACE METHODOLOGY

4. Response surface methodology

Response surface methodology is very useful and modern technique for the prediction and optimization of machining performances. In the present study, the strength of ABS material part made by fused deposition modelling machine has been predicted and also process parameters have been optimized by RSM. In this chapter, overview of RSM has been discussed. Response surface methodology (RSM) is a collection of statistical and mathematical techniques useful for developing, improving, and optimizing processes. The most extensive applications of RSM are in the particular situations where several input variable potentially influence some performance measure or quality characteristic of the process. This performance measure or quality characteristic is called the response. The input variables are sometimes called independent variables. The field of response surface methodology consists of the experimental strategy for exploring the space of the process or independent variables, Empirical statistical modelling to develop an approximated relationship between the yield and the process variables. Also, with the help of response surface methodology, optimization can be done for finding the values of the process variables that produce desirable values of the response [16].

In general, the relationship between the response y and independent variables ξ_1, ξ_2, …., ξ_k is,

$$Y= f(\xi_1,\xi_2,\ldots\ldots\ldots\ldots\xi_k) + \varepsilon \qquad \ldots\ldots\ldots\ldots\ldots\ldots\ldots\ldots(4.1)$$

where ε includes effects such as measurement error on the response, background noise, the effect of other variables, and so on. Usually ε is treated as a statistical error, often assuming it to have a normal distribution with mean zero and variance σ^2. Then,

$$E(y) = \eta = E[f(\xi_1,\xi_2,\ldots\ldots\ldots\xi_k)] + E(\varepsilon) = f(\xi_1, \xi_2,\ldots\ldots\ldots..\xi_k) \qquad \ldots\ldots\ldots\ldots\ldots...(4.2)$$

The variables $\xi_1, \xi_2, \ldots, \xi_k$ in equation (4.2) are usually called the natural variables, because they are expressed in the natural units of measurement, such as degrees Celsius, pounds per square inch, etc. In much RSM work, it is convenient to transform the natural variables to coded variables $x_1, x_2, \ldots, x_k$, which are usually defined to be dimensionless with mean zero and the same standard deviation. In terms of the coded variables, the response function equation (4.2) can be written as,

$$\eta = f(x_1, x_2 \ldots\ldots\ldots x_k) \qquad \ldots\ldots\ldots\ldots\ldots\ldots\ldots\ldots\ldots\ldots (4.3)$$

Because the form of the true response function is unknown, it should be approximated. In fact, successful use of RSM is critically dependent upon the experimenter's ability to develop a suitable approximation. Usually, a low-order polynomial in some relatively small region of the independent variable space is appropriate. In many cases, either a first-order or a second-order model is used. The first-order model is likely to be appropriate when the experimenter is interested in approximating the true response surface over a relatively small region of the independent variable space in a location where there is little curvature in response function. For the case of two independent variables, the first-order model in terms of the coded variables is given by,

$$\eta = \beta_0 + \beta_1 x_1 + \beta_2 x_2 \qquad \ldots\ldots\ldots\ldots\ldots\ldots\ldots\ldots\ldots\ldots (4.4)$$

The form of the first-order model in equation (4.4) is sometimes called a main effects model, because it includes only the main effects of the two variables x_1 and x_2. If there is an interaction between these variables, it can be added to the model easily as expressed below:

$$\eta = \beta_0 + \beta_1 x_1 + \beta_2 x_2 + \beta_{12} x_1 x_2 \qquad \ldots\ldots\ldots\ldots\ldots\ldots\ldots\ldots\ldots\ldots (4.5)$$

This is the first-order model with interaction. Adding the interaction term introduces curvature into the response function. Often the curvature in the true response surface is strong enough that the first-order model (even with the interaction term included) is inadequate. A second-order model will likely be required in these situations. For the case of two variables, the second-order model is:

$$\eta = \beta_0 + \beta_1 x_1 + \beta_2 x_2 + \beta_{11} x^2_1 + \beta_{22} x^2_2 + \beta_{12} x_1 x_2 \quad \text{.....} (4.6)$$

This model would likely be useful as an approximation to the true response surface in a relatively small region.

The second-order model is widely used in response surface methodology for several reasons:

- the second-order model is very flexible. It can take on a wide variety of functional forms, so it will often work well as an approximation to the true response surface.
- It is easy to estimate the parameters in the second-order model. The method of least Squares can be used for this purpose.
- There is considered to be practical experience indicating that second-order models work well in solving real response surface problems. In general, the first-order model is:

$$\eta = \beta_0 + \beta_1 x_1 + \beta_2 x_2 + \ldots\ldots\ldots\ldots + \beta_k x_k \quad \text{.....} (4.7)$$

And the second-order model is

$$\eta = \beta_0 + \sum_{j=1}^{k} \beta_j x_j + \sum_{j=1}^{k} \beta_{jj} x_j^2 + \sum_k \sum_{j=2}^{k} \beta_{ij} x_i x_j \quad \text{.....} (4.8)$$

Finally, it should be noted that there is a close connection between RSM and linear regression analysis. For example, say, the following model is considered:

$$\eta = \beta_0 + \beta_1 x_1 + \beta_2 x_2 + \ldots\ldots\ldots\ldots + \beta_k x_k + \varepsilon \quad \text{.....} (4.9)$$

The β's are a set of unknown parameters. To estimate the values of these parameters, the experimental data must be needed.

4.1. Response Surface Methodology and Robust Design:

RSM is an important branch of experimental design. It is also a critical technology in developing new processes and optimizing their performance. The objectives of quality improvement, including reduction of variability and improved process and product performance, can often be accomplished directly using RSM. It is well known that variation in key performance characteristics can result in poor process and product quality. During the 1980s, considerable attention was given to process quality, and methodology was developed for using experimental design, specifically for the following:

- For designing or developing products and processes so that they are robust to component variation.
- For minimizing variability in the output response of a product or a process around a target value.
- For designing products and processes so that they are robust to environment conditions.
- By robust means that the product or process performs consistently on target and is

relatively insensitive to factors that are difficult to control.

Professor Genichi Taguchi used the term robust parameter design (RPD) to describe his approach to this important problem. Essentially, robust parameter design prefers to reduce process or product variation by choosing levels of controllable factors (or parameters) that make the system insensitive (or robust) to changes in a set of uncontrollable factors. These uncontrollable factors represent most of the sources of variability. Taguchi referred to these uncontrollable factors as noise factors. In RSM, it is assumed that these noise factors are

uncontrollable in the field, but can be controlled during process development for purposes of a designed experiment.

Considerable attention has been focused on the methodology advocated by Taguchi, and a number of flaws in his approach have been discovered. However, the framework of response surface methodology allows easily incorporate many useful concepts in his philosophy.

4.2 The Sequential Nature of the Response Surface Methodology:

Most applications of RSM are sequential in nature. They are briefly discussed below:

Phase 0: At first, some ideas should be generated concerning which factors or variables are likely to be important in response surface study. It is usually known as a screening experiment. The objective of factor screening is to reduce the list of candidate variables to a relatively few so that subsequent experiments will be more efficient and require fewer runs or tests. The purpose of this phase is the identification of the important independent variables.

Phase 1: The objective of the experiment is to determine if the current settings of the independent variables result in a value of the response that is near the optimum. If the current settings or levels of the independent variables are not consistent with optimum performance, then a set of adjustments must be done to the process variables that will move the process toward the optimum. This phase of RSM makes considerable use of the first-order model and an optimization technique called the method of steepest ascent /descent.

Phase 2: When the process is near the optimum, it is required to develop a model that will accurately approximate the true response function within a relatively small region around the optimum. As the true response surface usually exhibits curvature near the optimum, a second-order model (or perhaps some higher-order polynomial) should be used. Once an appropriate approximated model has been obtained, this model may be analyzed to determine the optimum

conditions for the process. This sequential experimental process is usually performed within some region of the independent variable space called the operability region or experimentation region or region of interest.

4.3 Building Empirical Models:

4.3.1 Linear regression model:

In the practical application of RSM, it is necessary to develop an approximated model for the true response surface. The true response surface is typically driven by some unknown physical mechanism. The approximated model is based on observed data from the process or system and it is an empirical model. Multiple regressions is a collection of statistical techniques useful for building the types of empirical models required in RSM.

The first-order multiple linear regression models with two independent variables is:

$$Y = \beta_0+\beta_1 x_1+\beta_2 x_2+\varepsilon \quad \text{……………………………………………(4.10)}$$

The independent variables are often called predictor variables or regressors. The term "linear" is used because equation (4.10) is a linear function of the unknown parameters β_0, β_1 and β_2.

In general, the response variable y may be related to k regressor variables. The model is given by:

$$Y = \beta_0+\beta_1 x_1+\beta_2 x_2 +\text{……..}+ \beta_k x_k+\varepsilon \quad \text{………………………………..(4.11)}$$

This is called a multiple linear regression model with k regressor variables. The parameters β_j, j=0,l, ...k, are called the regression coefficients. Models those are more complex in appearance than equation (4.11) may often be analyzed by multiple linear regression techniques. For example, adding an interaction term to the first-order model in two variables, the model becomes:

$$Y= \beta_o+\beta_1 x_1+\beta_2 x_2+\beta_{12} x_1 x_2+\varepsilon \quad \text{……………………..………………(4.12)}$$

As another example, considering the second-order response surface model in two variables, the model becomes:

$$\eta = \beta_0 + \beta_1 x_1 + \beta_2 x_2 + \beta_{11} x^2_1 + \beta_{22} x^2_2 + \beta_{12} x_1 x_2 + \varepsilon \qquad \text{……………………(4.13)}$$

In general, any regression model that is linear in the parameters (the β-values) is a linear regression model, regardless of the shape of the response surface that it generates.

4.3.2 Estimation of the parameters in linear regression models:

The method of least squares is typically used to estimate the regression coefficients in a multiple linear regression model. It is, say, supposed that $n > k$ observations on the response variable are available: $y_1, y_2, \ldots, y_n$. Along with each observed response y_i, each regressor variable has to be observed, x_{ij} denotes the i-th observation or level of variable x_j. The model in terms of the observations may be written in matrix notation as:

$$y = X\beta + \varepsilon \qquad \text{……………………………………(4.14)}$$

Where,

y is an n x 1 vector of the observations,

X is an n x p matrix of the levels of the independent variables,

β is a p x 1 vector of the regression coefficients, and

ε is an n x 1 vector of random errors.

It is required to find the vector of least squares estimators, b, that minimizes:

$$L = \sum_{i=1}^{n} \varepsilon_1^2 = \varepsilon'\varepsilon = (y - X\beta)'(y - X\beta) \qquad \text{………………………….……....(4.15)}$$

After some simplifications, the least squares estimator of β is:

$$b = (x'x)^{-1} x'y \qquad \text{…………………………………(4.16)}$$

It is easy to see that X'X is a p x p symmetric matrix and X'y is a p x 1 column vector. The matrix X'X has the special structure. The diagonal elements of X'X are the sums of squares of

the elements in the columns of X, and the off-diagonal elements are the sums of cross-products of the elements in the columns of X. Furthermore, the elements of X'y are the sums of cross-products of the columns of X and the observations {yi}.

The fitted regression model is:

$$\hat{Y}=Xb \qquad \text{……..(4.17)}$$

The difference between the observation y_i and the fitted value is a residual,

$$e_i = y_i - \hat{Y} \qquad \text{……..(4.18)}$$

The n x 1 vector of residuals is denoted by:

$$e = y - \hat{Y} \qquad \text{……(4.19)}$$

4.3.3 Model adequacy checking:

It is always necessary to

- Examine the fitted model to ensure that it provides an adequate approximation to the true system.
- Verify that none of the least squares regression assumptions are violated.

4.3.4 Properties of the least square estimators:

The method of least squares produces an unbiased estimator of the parameter β in the multiple linear regression models. The important parameter is the sum of squares of the residuals

$$SS_E = \sum_{i=1}^{n} (y_i-\hat{Y}_i)^2 = \sum_{i=1}^{n} e_i^2 = e'e \qquad \text{…….……(4.20)}$$

Because X'Xb = X'y, a computational formula for SSE can be derived as:

$$SS_E = y'y - b'X'y \qquad \text{……(4.21)}$$

Equation (4.21) is called the error or residual sum of squares.

It can be shown that an unbiased estimator of σ^2 is:

$$\sigma^2 = \frac{SS_E}{n-p} \qquad \text{.....(4.22)}$$

Where,

n is a number of observations and

p is a number of regression coefficients.

The total sum of squares is:

$$SS_T = y'y - \frac{(\sum_{i=1}^{n} y_i)^2}{n} = \sum_{i=1}^{n} y_i^2 - \frac{(\sum_{i=1}^{n} y_i)^2}{n} \qquad \text{.....(4.23)}$$

Then the coefficient of multiple determination R^2 is defined as:

$$R^2 = 1 - \frac{SS_E}{SS_T} \qquad \text{.....(4.24)}$$

R^2 is a measure of the amount of reduction in the variability of y obtained by using the regressor variables $x_1, x_2, ..., x_k$ in the model. From inspection of the analysis of variance identity equation (Equation (4.24)) can see that $0 \le R^2 \le 1$ However, a large value of R^2 does not necessarily imply that the regression model is good one. Adding a variable to the model will always increase R^2, regardless of whether the additional variable is statistically significant or not. Thus it is possible for models that have large values of R^2 to yield poor predictions of new observations or estimates of the mean response.

Because R^2 always increases as terms are added to the model, it is preferable to use an adjusted R^2 statistic defined as:

$$R_{adj}^2 = \frac{SS_E/(n-p)}{SS_T/(n-1)} = 1 - \frac{(n-1)}{(n-p)}(1-R^2) \qquad \text{.....(4.25)}$$

In general, the adjusted R^2 statistic will not always increase as variables are added to the model. In fact, if unnecessary terms are added, the value of R^2_{adj} will often decrease. When R^2

and R^2_{adj} differ dramatically, there is a good chance that non significant terms have been included in the model.

However, testing hypotheses on the individual regression coefficients are very much important. Such tests would be useful in determining the value of each of the regressor variables in the regression model. For example, the model might be more effective with the inclusion of additional variables, or perhaps with the deletion of one or more of the variables already in the model.

Adding a variable to the regression model always causes the sum of squares for regression to increase and the error sum of squares to decrease. It must be decided whether the increase in the regression sum of squares is sufficient to warrant using the additional variable in the model. Furthermore, adding an unimportant variable to the model can actually increase the mean square error, thereby decreasing the usefulness of the model [17].

4.3.5 Residual analysis:

The residuals from the least squares fit, defined by $e_i = y_i - \hat{y}_i$, $i = 1, 2,..., n,$ play an important role in judging model adequacy. It is preferable to work with scaled residuals, in contrast to the ordinary least squares residuals. These scaled residuals often convey more information than do the ordinary residuals. The standardizing process scales the residuals by dividing them by their average standard deviation. In some data sets, residuals may have standard deviations that differ greatly. There is some other way of scaling that takes this into account. The vector of fitted values $\hat{y}_I$ corresponding to the observed values y_i is

$$\hat{Y} = Xb = X(X'X)^{-1} X'y = Hy \qquad \text{.....(4.26)}$$

The n x n matrix $H = X(X'X)^{-1} X'$ is usually called the hat matrix because it maps the vector of observed values into a vector of fitted values. The hat matrix and its properties play a central role in regression analysis.

$$e = y - Xb = y - Hy = (1-H)y \qquad \ldots\ldots\ldots\ldots\ldots\ldots\ldots\ldots\ldots\ldots \quad (4.27)$$

The prediction error sum of squares provides a useful residual scaling:

$$\text{PRESS} = \sum_{i=1}^{n} \left(\frac{e_i}{1-h_{ii}}\right)^2 \qquad \ldots\ldots\ldots\ldots\ldots\ldots \quad (4.28)$$

From Equation (5.28) it is easy to see that the PRESS residual is just the ordinary residual weighted according to the diagonal elements of the hat matrix h_{ii}. Generally, a large difference between the ordinary residual and the PRESS residual will indicate a point where the model fits the data well, but a model built without that point predicts poorly.

4.4 Variable Selection and Model Building in Regression:

In response surface analysis, it is customary to fit the full model corresponding to the situation at hand. It means that in steepest ascent, the full first-order model is usually fitted, and in the analysis of the second-order model, the full quadratic is usually fitted. Nevertheless, in some cases, where the full model may not be appropriate; that is, a model based on a subset of the regressors in the full model may be superior. Variable selection or model-building techniques usually is used to identify the best subset of regressors to include in a regression model Now, it is assumed that there are K candidate regressors denoted $x_1, x_2, \ldots, x_k$ and a single response variable y. All models will have an intercept term β_0, so that the full model has (K + 1) parameters. It is shown that there is a strong motivation for correctly specifying the regression model: Leaving out important regressors introduces bias into the parameter estimates, while including unimportant variables weakens the prediction or estimation capability of the model.

4.4.1 Procedures for variable selection:

Now, it is required to find several of the more widely used methods for selecting the appropriate subset of variables for a regression model. The approach is also made on the optimization procedure used for selecting the best model from the whole set of models and finally it is required to discuss and illustrate several of the criteria that are typically used to decide which subset of the candidate regressors leads to the best model.

4.4.2 All possible regression:

This procedure requires that all the regression equations are fitted involving one-candidate regressors, two-candidate regressors, and so on. These equations are evaluated according to some suitable criterion, and the best regression model selected. If it is assumed that the intercept term β_0 is included in all equations, then there are K candidate regressors and there are 2^K total equations to be estimated and examined. For example, if K = 4, then there are 2^4= 16 possible equations, whereas if K = 10, then there are2^{10} = 1024. Clearly the number of equations to be examined increases rapidly as the number of candidate regressors increases. Usually, the candidate variables are restricted for the model to those in the full quadratic polynomial and it is required that all models obey the principal of hierarchy. A model is said to be hierarchical if the presence of higher-order terms (such as interaction and second-order terms) requires the inclusion of all lower-order terms contained within those of higher order. For example, this would require the inclusion of both main effects, if a two-factor interaction term was in the model. Many regression model builders believe that hierarchy is a reasonable model-building practice while fitting polynomials.

4.4.3 Stepwise regression methods:

As the evaluation of all possible regressions can be burdensome, various methods have been developed for evaluating only a small number of subset regression models by either adding or deleting regressors one at a time. These methods are generally referred to as stepwise-type procedures. They can be classified into three broad categories:

a) Forward selection,

b) Backward elimination, and

c) Stepwise regression, which is a popular combination of procedures (a) and (b).

a) Forward selection:

This procedure begins with the assumption that there are no regressors in the model other than the intercept. An effort is made to find an optimal subset by inserting regressors into the model one at a time. The first regressor selected for entry into the equation is the one that has the largest simple correlation with the response variable y. If it is supposed that the first regressor is x_1, then the regressor will produce the largest value of the F-statistic for testing significance of regression. This regressor is entered, if the F-statistic exceeds a pre-selected F-value, say, F_{in} (or F-to-enter). The second regressor chosen for entry is the one that now has the largest correlation with y after adjusting for the effect of the first regressor entered (x_1) on y. It is referred as partial correlations. In general, at each step the regressor having the highest partial correlation with y (or equivalently the largest partial F-statistic given the other regressors already in the model) is added to the model, if its partial F-statistic exceeds the pre-selected entry level F_{in}. The procedure terminates either when the partial F-statistic at a particular step does not exceed F_{in} or when the last candidate regressor is added to the model.

b) Backward elimination:

Forward selection begins with no regressors in the model and attempts to insert variables until a suitable model is obtained. Backward elimination attempts to find a good model by working in the opposite direction. That is, it is required to start a model that includes all K Candidate regressors. Then the partial F-statistic (or a t-statistic, which is equivalent) is computed for each regressor, as if, it were the last variable to enter the model. The smallest of these partial F-statistics is compared with a pre-selected value, F_{out} (or F-to-remove); and if the smallest partial F-value is less than F_{out}, that regressor is removed from the model. Now, a regression model with (K – 1) regressors is fitted, the partial F-statistic for this new model calculated, and the procedure repeated. The backward elimination algorithm terminates, when the smallest partial F-value is not less than the pre-selected cut-off value F_{out}.

c) Stepwise regression:

The two procedures described above suggest a number of possible combinations. One of the most popular is the stepwise regression algorithm. This is a modification of forward selection in which at each step all regressors, entered into the model previously, are reassessed via their partial F-or t-statistics. A regressor added at an earlier step may now be redundant because of the relationship between it and regressors now in the equation. If the partial F-statistic for a variable is less than F_{out}, that variable is dropped from the model. Stepwise regression requires two cut-off values, F_{in} and F_{out}. Sometimes, it is preferred to choose $F_{in} = F_{out}$, although this is not necessary. Sometimes, it is also chosen that $F_{in} > F_{out}$, making it more difficult to add a regressor than to delete one. In the present study, some of the concepts of RSM have been used for predicting the FDM response viz, Tensile Strength, Flexural strength, and Impact strength. Also, the optimization of process parameters has been done by RSM.

CHAPTER 5

SPECIMEN PREPARATION,

EXPERIMENT AND ANALYS

5.1. Specimen preparation

Tensile test specimens having dimensions 60 mm x 20 mm x 5 mm. Flexural test specimens were 80 mm x 10 mm x 4 mm, and impact test specimens 80 mm x 10 mm x 4 mm, and V notch of radius 0.25 mm. Since orientation is an important parameter for part strength, tests have been conducted by changing the orientation for measuring Tensile strength (ASTMD 638), Flexural strength (ASTMD 790) and Impact strength (ASTM D256). The part are modeled in CATIAV5 software and exported as STL file. STL file is imported to FDM software (Insight). Here, factors are set as per experiment plan. Three parts per experiment are fabricated using FDM Vantage SE machine[18]. The material use for part fabrication is ABS P400. Parts are modeled and experiment is conducted as per ISO R527:1966, ISO 178:1975 and ISO 180:1982 for tensile, flexural and impact tests respectively. And part made according to response surface design 32 runs.

Table 5.1 Domain of experiments

Factor	Symbol	Unit	Level				
			Lowest(-2)	Low(-1)	Middle(0)	High(1)	Highest(2)
Layer thickness	A	Mm	0.127	0.158	0.190	0.222	0.254
Sample orientation	B	degree	0	15	30	45	60
Raster angle	C	degree	0	15	30	45	60
Raster width	D	Mm	0.4064	0.4264	0.4464	0.4664	0.4864
Air gap	E	Mm	0	0.002	0.004	0.006	0.008

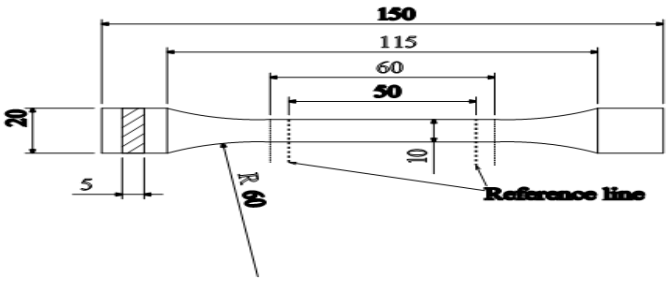

Figure 5.1 Line diagram of specimen for tensile test

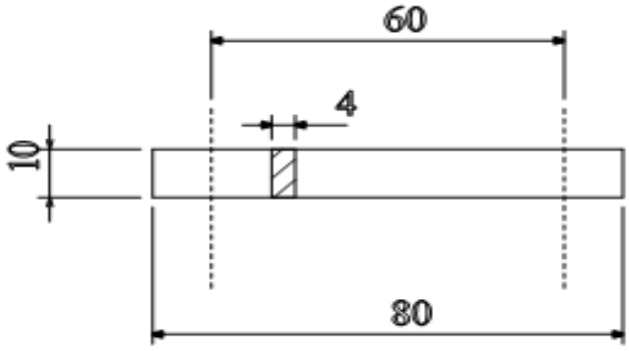

Figure 5.2 Line diagram of specimen for flexural test

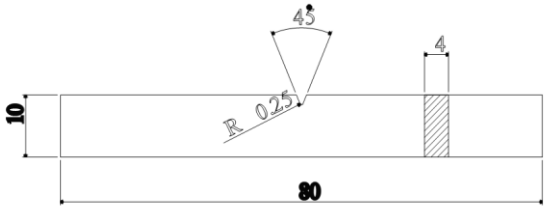

Figure 5.3 Line diagram of specimen for izod test

After making the test specimen According to response surface design 32 runs on the FDM Vantage SE (RP) machine, these specimens were tested. Tensile test and 3-point bending test

(flexural test) were conducted on Instron 1195 machine and Impact test was on Instron - Wolpert Pendulum Impact Testing Machine.

5.2. Testing of specimens:

Tensile strength at break is determined according to ISO R527:1966. Shows the shape of the test specimens. Flexural strength at yield of test specimen is determined as per ISO R178:1975 standard. Three point bending test is used for flexural strength determination. For this specimen is supported by two supports and loaded in the middle by force, until the test specimen fractures [19]. The tensile testing and three-point bending tests were performed using an Instron 1195 series IX automated material testing system with crosshead speeds of 1mm/s and 2mm/s respectively. Charpy impact test performed in Instron Wolpert pendulum impact test machine is used to determine the impact strength of specimen as per ISO/179:1982. During impact testing specimen is subjected to quick and intense blow by hammer pendulum striking the specimen with a speed of 3.8 m/s. The impact energy absorbed is measure of the toughness of material and it is calculated by taking the difference in potential energies of initial and final position of hammer.

following condition were taken during the different test:

Machine parameter of Instron 1195 tensile test:

Sample type	:	ASTM
Sample rate (pts/sec)	:	9.103
Cross head speed (mm/min)	:	1.000
Full scale loading range(KN)	:	20.00
Humidity (%)	:	50%
Temperature (deg.F)	:	73

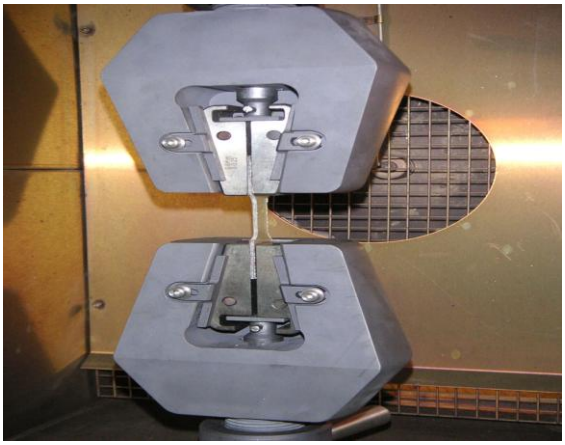

(a) Figure of tensile test

(b) specimen after fracture

Figure 5.4 Instron test of tensile specimen

Machine parameter of Instron 1195 flexural test :

Sample type	:	ASTM
Sample rate (pts/sec)	:	9.103
Cross head speed(mm/min)	:	2.00
Full scale load range (KN)	:	5.00
Humidity (%)	:	50%
Temperature (deg. F)	:	73

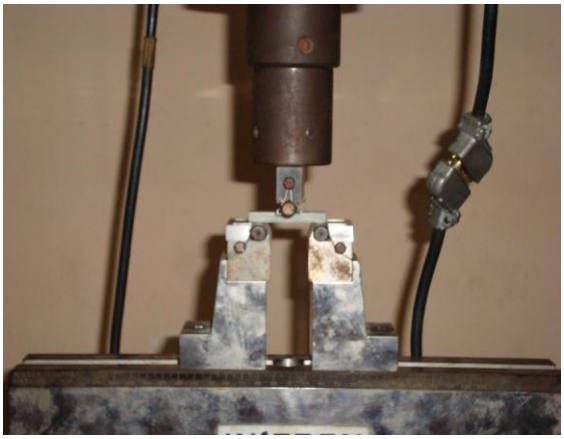

(c) Figure of flexural test

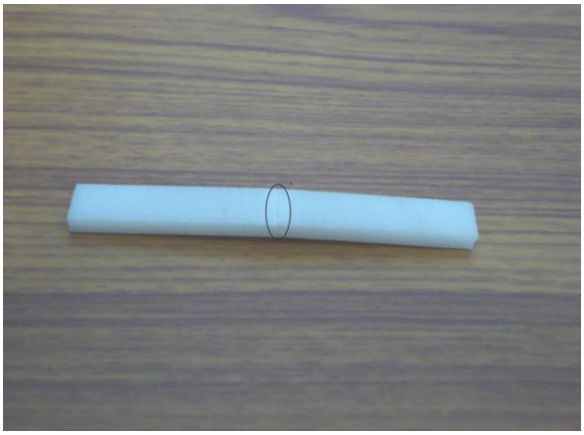

(d) Specimen after bending

Figure 5.5 3-point bending test of specimen

Machine parameter Instron - Wolpert Pendulum Impact Testing Machine:

Sample type	:	ASTM
Impact test striking velocity	:	3.8 m/sec
Pendulum fall angle	:	160^{o}
pendulum fall height	:	0.757 m
length of pendulum	:	390 mm

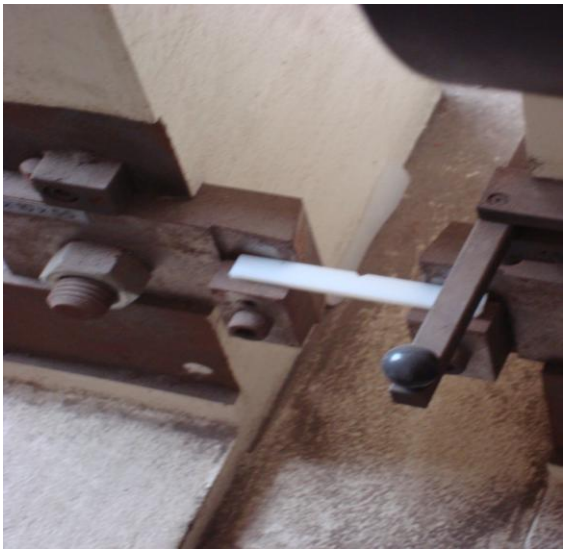

(e) Figure of impact test

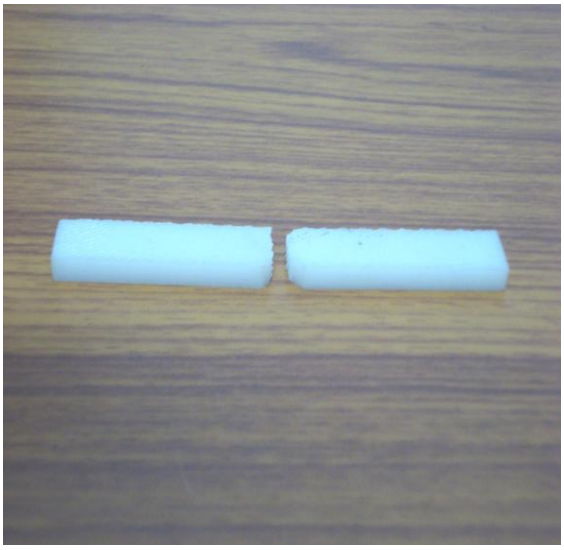

(f) specimen after break

Figure 5.6 Impact test of specimen

In order to build empirical model for Tensile strength, flexural strength and impact strength, experiments were conducted based on central composite design (CCD). The CCD is capable of fitting second order polynomial and is preferable if curvature is assumed to be present in the system. To reduce the experiment run, half factorial (two levels) is considered. Maximum and minimum value of each factor is coded into +2 and -2 respectively using, so that all input factors are represented in same range [17].

$$\xi_{ij} = 2 \times \frac{x_{ij} - (x_{i,max}+x_{i,min})/2}{(x_{i,max}-x_{i,min})/2}$$

where ξ_{ij} and x_{ij} are coded and actual value of j^{th} level of i^{th} factor respectively.

Table 5.2 Experimental data obtained from the CCD runs

Run Order	Factor(coded units)					Tensile strength (MPa)	Flexural strength (MPa)	Impact strength (Joules)
	A	B	C	D	E			
1	-1	-1	-1	-1	1	11.54	31.70	11.80
2	1	-1	-1	-1	-1	17.76	31.40	11.30
3	-1	1	-1	-1	-1	11.04	25.00	10.50
4	1	1	-1	-1	1	13.69	26.50	14.00
5	-1	-1	1	-1	-1	12.29	31.90	10.85
6	1	-1	1	-1	1	12.35	42.00	11.35
7	-1	1	1	-1	1	11.15	32.10	12.85
8	1	1	1	-1	-1	12.29	38.80	11.60
9	-1	-1	-1	1	-1	16.73	30.10	10.79
10	1	-1	-1	1	1	16.17	31.60	13.80
11	-1	1	-1	1	1	11.04	29.70	10.90
12	1	1	-1	1	-1	11.86	19.20	11.90
13	-1	-1	1	1	1	12.94	31.80	12.80
14	1	-1	1	1	-1	15.60	31.90	10.40
15	-1	1	1	1	-1	11.05	35.70	11.70
16	1	1	1	1	1	16.31	34.00	11.37
17	-2	0	0	0	0	11.14	39.70	11.50
18	2	0	0	0	0	16.10	39.10	12.14
19	0	-2	0	0	0	16.55	32.00	10.80
20	0	2	0	0	0	11.04	24.20	12.30
21	0	0	-2	0	0	15.60	21.30	13.40
22	0	0	2	0	0	12.30	34.20	12.30
23	0	0	0	-2	0	12.26	37.50	11.40
24	0	0	0	2	0	16.40	36.00	12.40
25	0	0	0	0	-2	13.98	39.70	11.50
26	0	0	0	0	2	12.40	39.80	14.30
27	0	0	0	0	0	15.20	42.20	14.90
28	0	0	0	0	0	16.30	40.10	15.50
29	0	0	0	0	0	15.90	41.60	14.70

30	0	0	0	0	0	16.40	41.10	15.00
31	0	0	0	0	0	15.50	42.30	15.10
32	0	0	0	0	0	15.90	41.80	14.90

5.3 Analysis of experiments:

Analysis of the experimental data obtained from CCD design runs is done on MINITAB R14 software using full quadratic response surface model as given by .

$$y = \beta_0 + \sum_{i=1}^{k} \beta_i x_i + \sum_{i=1}^{k} \beta_{ii} x_i x_i + \sum_{i<j} \sum \beta_{ij} x_i x_j$$

Where y is the response, x_i is i^{th} factor

For significance check F value given in ANOVA table is used. Probability of F value greater than calculated F value due to noise is indicated by p value. If p value is less than 0.05, significance of corresponding term is established. For lack of fit p value must be greater the 0.05. An insignificant lack of fit is desirable as it indicates anything left out of model is not significant and develop model fits.

Based on analysis of variance (ANOVA) test full quadratic model was found to be suitable for tensile strength, flexural strength and impact strength with regression p-value less than 0.05 and lack of fit more then 0.05.

5.3.1 Analysis of experiment for tensile test:

Table 5.3 Estimated regression coefficients for tensile test

Term	Coef.	SE Coef.	T	P
Constant	15.8469	0.2408	65.814	0.000
A	1.1737	0.1232	9.525	0.000
B	-1.1654	0.1232	-9.458	0.000
C	-0.5188	0.1232	-4.210	0.001
D	-0.7446	0.1232	6.042	0.000
E	-0.2746	0.1232	-2.228	0.048
A*A	-0.5419	0.1115	-4.862	0.001
B*B	-0.4982	0.1115	-4.470	0.001
C*C	-0.4594	0.1115	-4.122	0.002

D*D	-0.3644	0.1115	-3.270	0.007
E*E	-0.6494	0.1115	-5.826	0.000
A*B	0.0931	0.1509	0.617	0.550
A*C	-0.0006	0.1509	-0.004	0.997
A*D	-0.1181	0.1509	-0.783	0.450
A*E	0.3406	0.1509	2.257	0.045
B*C	0.7619	0.1509	5.048	0.000
B*D	-0.3381	0.1509	-2.240	0.047
B*E	0.9581	0.1509	6.349	0.000
C*D	0.3781	0.1509	2.505	0.029
C*E	0.4044	0.1509	2.679	0.021
D*E	0.3669	0.1509	2.431	0.033

S =0.6037 R^2 = 97.4% R^2 (adj) = 92.7%

In tensile test analysis all the factors and interaction A*A, B*B, C*C, D*D, E*E, A*E, B*C, B*D, B*E, C*D, C*E, and D*E interactions are important because their P value is less than 0.05. The coefficient of determination (R^2) which indicates the goodness of fit for the model so the value of R^2 =97.4% which indicate the high significance of the model.

With the above analysis we found the following regression equation:-

Ts = 15.8469+1.1737A -1.1654B -0.5188C +0.7446D -0.2746E -0.5419(A*A) - 0.4982(B*B) - 0.4594(C*C) -0.3644(D*D) - 0.6494(E*E) + 0.3406(A*E) +0.7619(B*C) – 0.3381(B*D) + 0.9581(B*E) + 0.3781(C*D) + 0.404(C*E) + 0.3669(D*E).

Table 5.4 Analysis of variance for tensile test

Source	DF	Tensile strength			
		SS	MS	F	p
Regression	20	151.522	7.5761	20.79	0.000
Linear	5	87.235	17.4470	47.87	0.000
Square	5	29.206	5.8413	16.03	0.000
Interaction	10	35.081	3.5081	9.63	0.000
Residual	11	4.009	0.3644		
Lack of fit	6	2.955	0.4926	2.34	0.185
Pure error	5	1.053	0.2107		
Total	31	155.530			

DF=degree of freedom SS= sum of square MS=mean sum of square

In the above table we can see P value of all the term is less than 0.05, so these all term are significant, and non significance lack of fit is desired in this case value of LOF is 0.185 which is more than 0.05 and non significant.

5.3.2 Response surface analysis for tensile test:

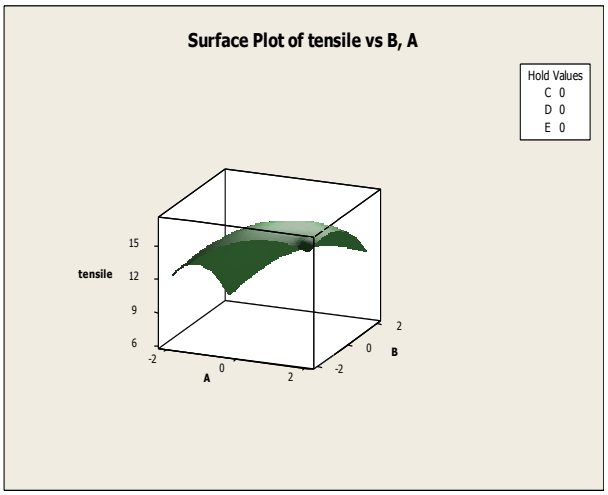

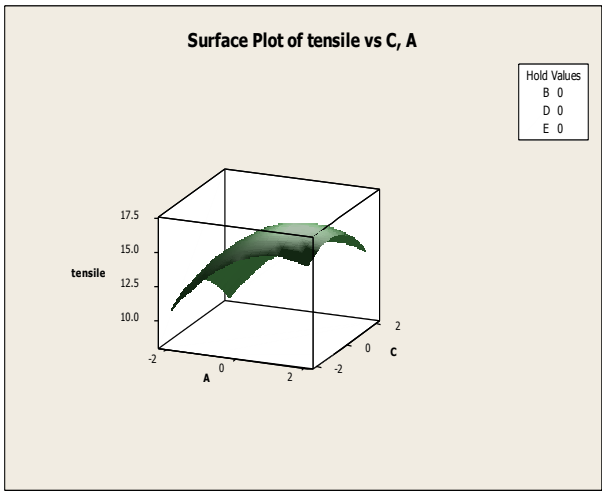

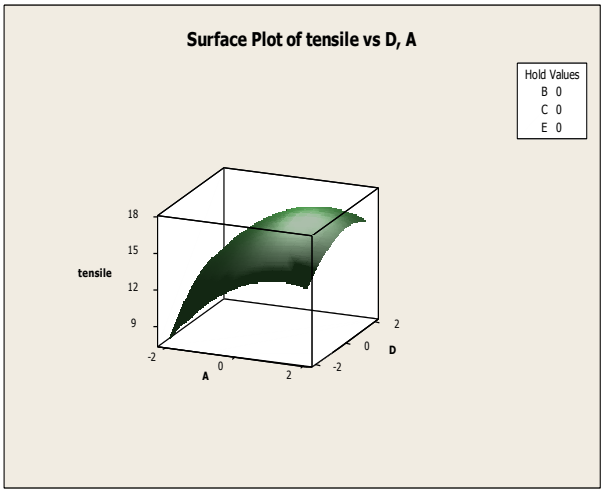

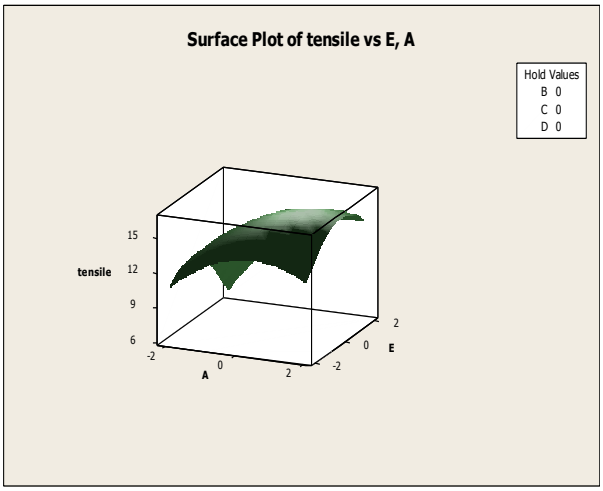

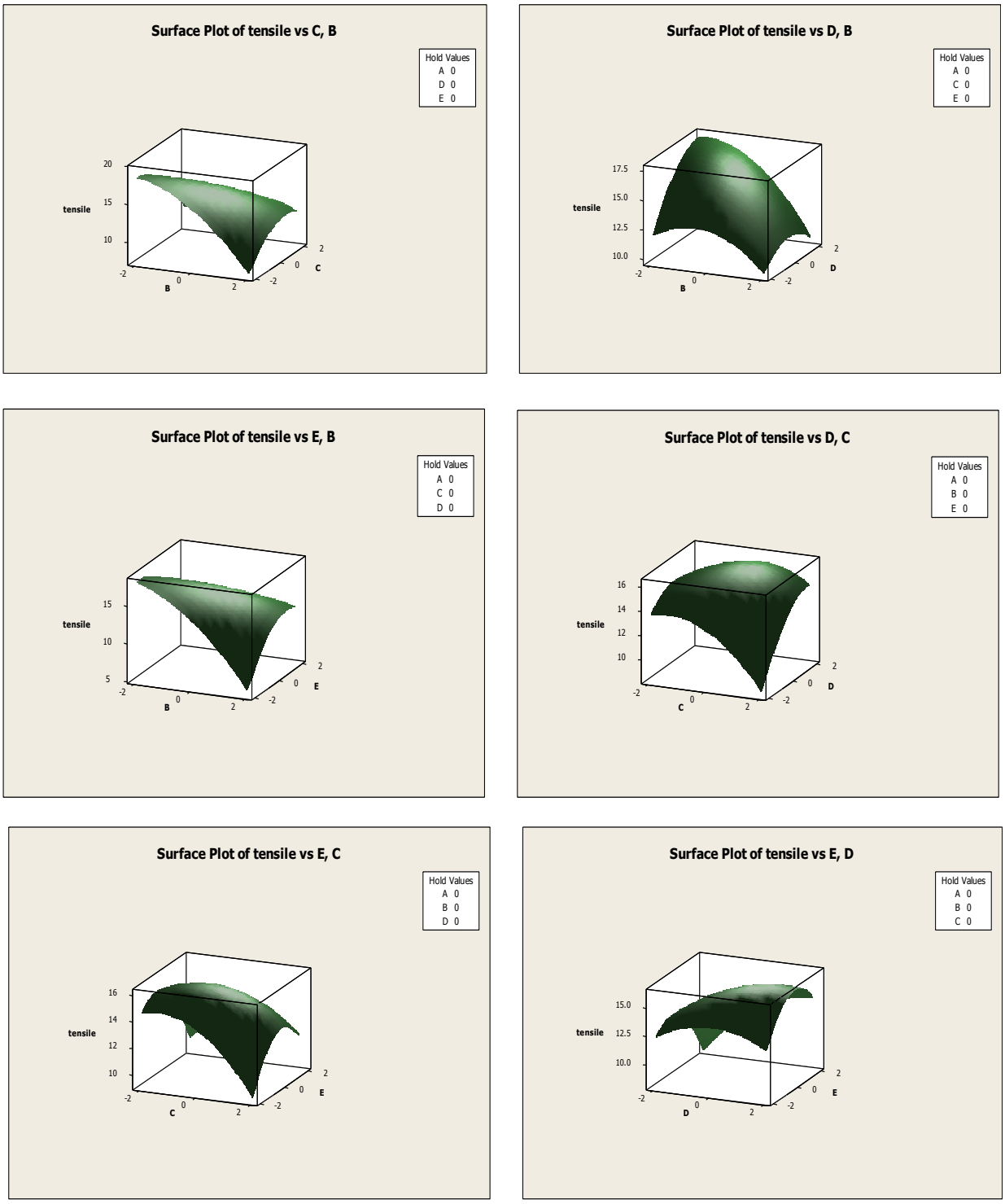

Figures 5.7 Surface plots for tensile strength

From response surface it is observed that strength first decrease and then increase with layer thickness (A) increase. The reason may be that at smaller layer thickness numbers of layers are more resulting in increase in heat conduction towards the bottom layers therefore strong bonding between adjacent rasters is expected. But this also increases the distortion in bottom layers which is responsible for weak bond strength, so with increase in layer thickness distortion in layer thickness decreased and tensile strength increased.

Response surface shows the decreasing trend of strength with respect to increase in orientation (B).this may be due to the stepped effect in which one layer does not coincide with the next layer exactly this ultimately reduce the strength of the part. Number of layers also increases with increase in orientation for same layer thickness as a result distortion in part will increase resulting in less bond strength.

Tensile strength is decreasing with respect to raster angle ,the reason may be that at small angle raster deposited have long length due to this inter bonding of the part is good and also number of layer is less. So, with increase in raster angle this inters bonding gets weak and decreases the strength.

Tensile strength is increase with increasing the raster width (D) , the reason may be that at small raster width number of layer are more so the distortion chances are higher, so with increase in raster width strength increase.

Tensile strength is increased up to certain level and after that level it decrease, this is due to that

If raster deposition is much closed the melt material can overlap to next raster and it can lose

Its strength. But this air gap should be maintain, if air gap is large there will be a gap between two raster and it can also reduce the strength.

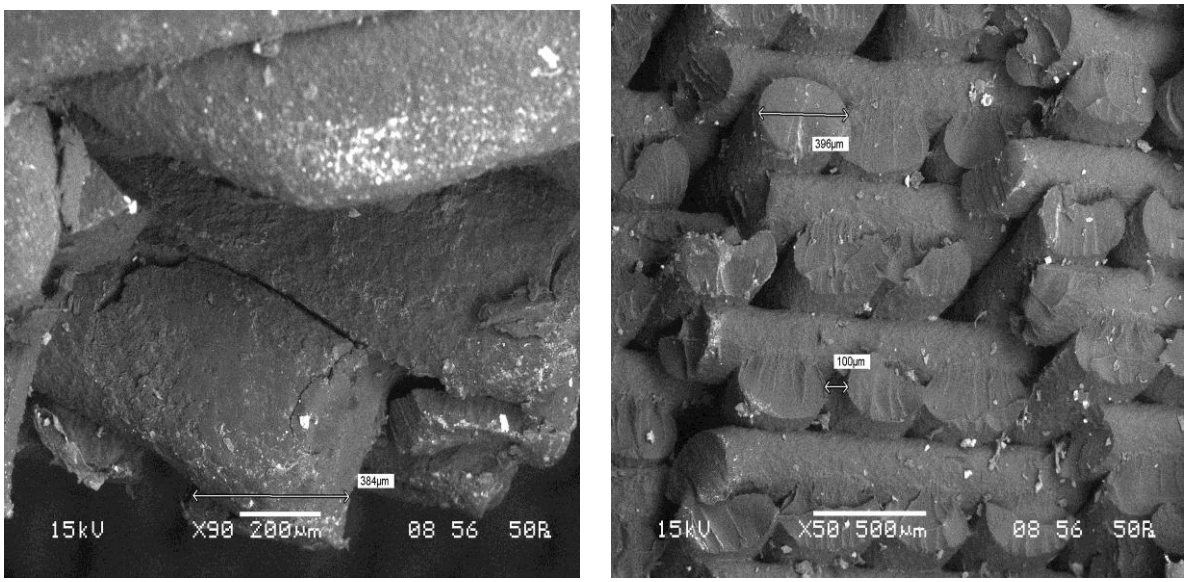

(a) Horizontal position of specimen (b) vertical position of specimen

Figure 5.8 SEM image of tensile failure of specimen

The above SEM images are shown for two position of tensile fracture (a) is a horizontal position of fractured specimen and (b) is vertical position of fractured specimen. We have 32 specimens for each test, so randomly we have chosen one specimen of parametric combination, and choose the specimen of parametric combination of 19 for the SEM image which will give the behavior of specimen after different test.

In Image (a) the circle portion shows the fracture on the specimen, This is the ABS P400 (acrylonitrile-butadine-styrene) material, and we can see there is no or negligible elongation in the specimen while we do the tensile test and material behavior like a brittle material and image (b) shows the different points from where fracture occurred.

5.3.3 Analysis of experiment for flexural test:

Table 5.5 Estimated regression coefficients for flexural test

Term	Coef.	SE Coef.	T	P
Constant	41.7159	0.5264	79.248	0.000
A	0.2583	0.2694	0.959	0.358
B	-1.5417	0.2694	-5.723	0.000
C	3.2833	0.2694	12.188	0.000
D	-0.7667	0.2694	-2.846	0.016
E	0.6500	0.2694	2.413	0.034
A*A	-0.7284	0.2437	-2.989	0.012
B*B	-3.5534	0.2437	-14.583	0.000
C*C	-3.6409	0.2437	-14.942	0.000
D*D	-1.3909	0.2437	-5.708	0.000
E*E	-0.6409	0.2437	-2.630	0.023
A*B	-0.9625	0.3299	-2.917	0.014
A*C	1.4375	0.3299	4.357	0.001
A*D	-1.7875	0.3299	-5.418	0.000
A*E	0.6375	0.3299	1.932	0.079
B*C	1.7125	0.3299	5.190	0.000
B*D	0.4875	0.3299	1.478	0.168
B*E	-0.5125	0.3299	-1.553	0.149
C*D	-0.4625	0.3299	-1.402	0.189
C*E	-0.7625	0.3299	-2.311	0.041
D*E	0.3125	0.3299	0.947	0.364

S = 1.320 R^2 = 98.5% R^2(adj) = 95.7%

In flexural test we can see by the above table factors B, C, D, E and interaction A*A, B*B, C*C, D*D, E*E, A*B, A*C, A*D, B*C, and C*E are most important because they are having P value less than 0.05.

The coefficient of determination (R^2) which indicates the goodness of fit for the model so the value of R^2 =98.5% which indicate the high significance of the model.

With the above analysis we found the following regression equation:-

Fs = 41.7159– 1.5417B + 3.2833C – 0.7667D + 0.6500E – 0.7284(A*A) – 3.5534 (B*B) – 3.6409 (C*C) – 1.3909 (D*D) – 0.6409 (E*E) – 0.9625 (A*B) + 1.4375(A*C) -1.7875 (A*D) + 1.7125(B*C) – 0.7625(C*E).

Table 5.6 ANOVA analysis for flexural test

Source	DF	Flexural strength			
		SS	MS	F	p
Regression	20	1238.44	61.922	35.55	0.000
Linear	5	341.62	68.323	39.23	0.000
Square	5	722.10	144.420	82.92	0.000
Interaction	10	174.73	17.473	10.03	0.000
Residual	11	19.16	1.742		
Lack of fit	6	15.81	2.635	3.94	0.077
Pure error	5	3.35	0.670		
Total	31	1257.60			

DF =degree of freedom SS = sum of square MS = mean sum of square

In the above table we can see P value of all the term is less than 0.05, so these all term are significant, and non significance lack of fit is desired in this case value of LOF is 0.077 which is more than 0.05 and non significant.

5.3.4 Response surface analysis for flexural test:

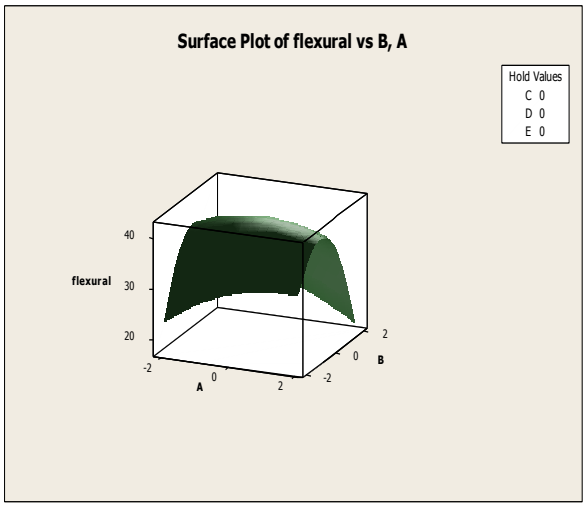

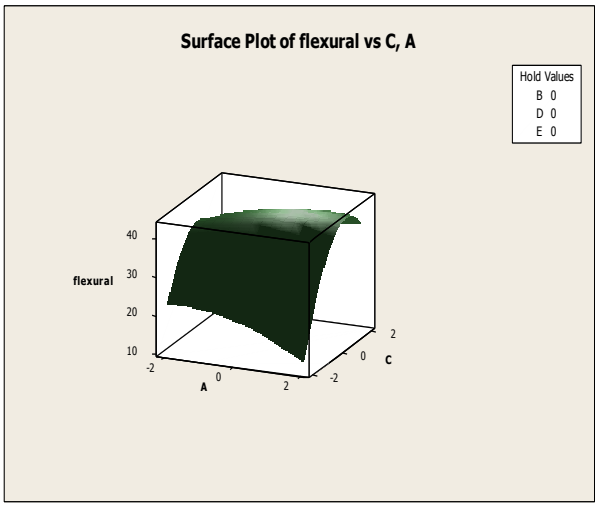

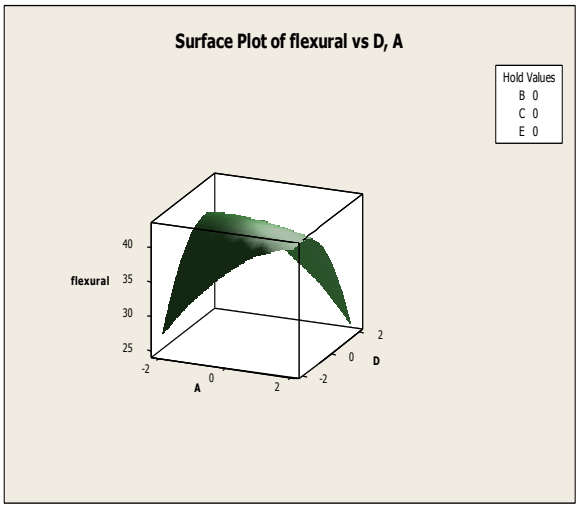
Surface Plot of flexural vs D, A
Hold Values
B 0
C 0
E 0
flexural
40
35
30
25
A
D
-2
0
2

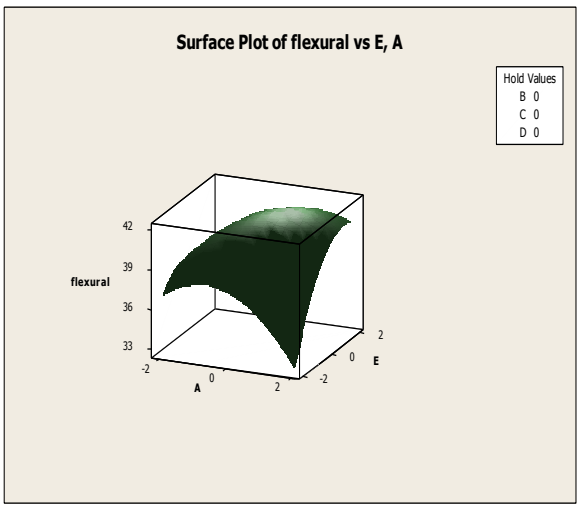
Surface Plot of flexural vs E, A
Hold Values
B 0
C 0
D 0
flexural
42
39
36
33
A
E
-2
0
2

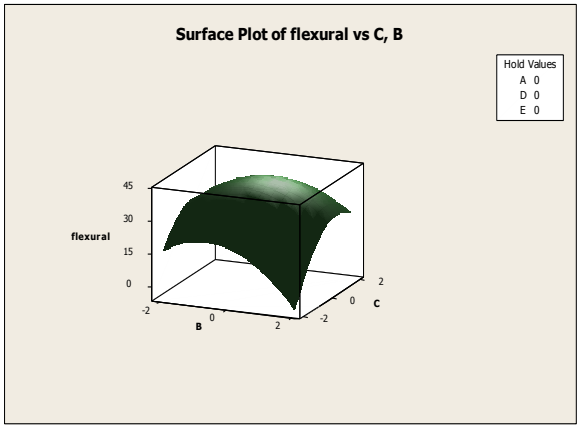
Surface Plot of flexural vs C, B
Hold Values
A 0
D 0
E 0
flexural
45
30
15
0
B
C
-2
0
2

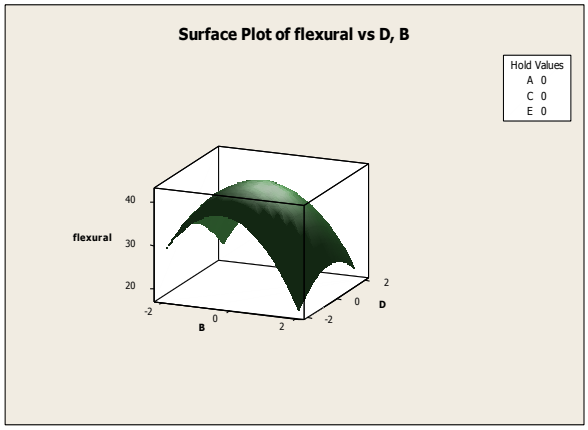
Surface Plot of flexural vs D, B
Hold Values
A 0
C 0
E 0
flexural
40
30
20
B
D
-2
0
2

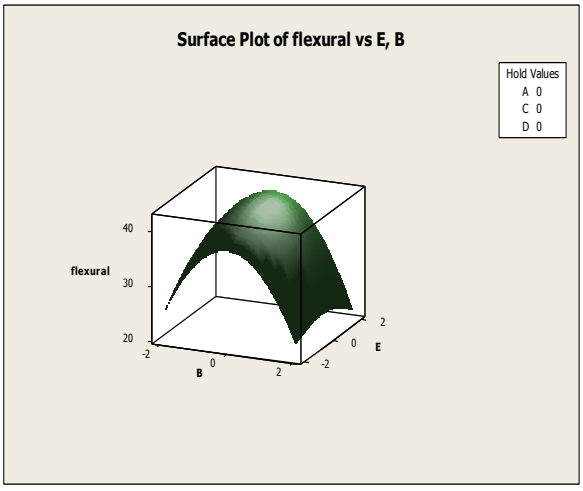
Surface Plot of flexural vs E, B
Hold Values
A 0
C 0
D 0
flexural
40
30
20
B
E
-2
0
2

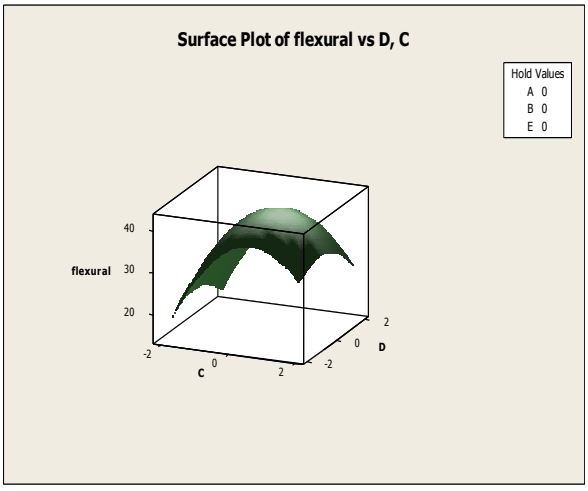
Surface Plot of flexural vs D, C
Hold Values
A 0
B 0
E 0
flexural
40
30
20
C
D
-2
0
2

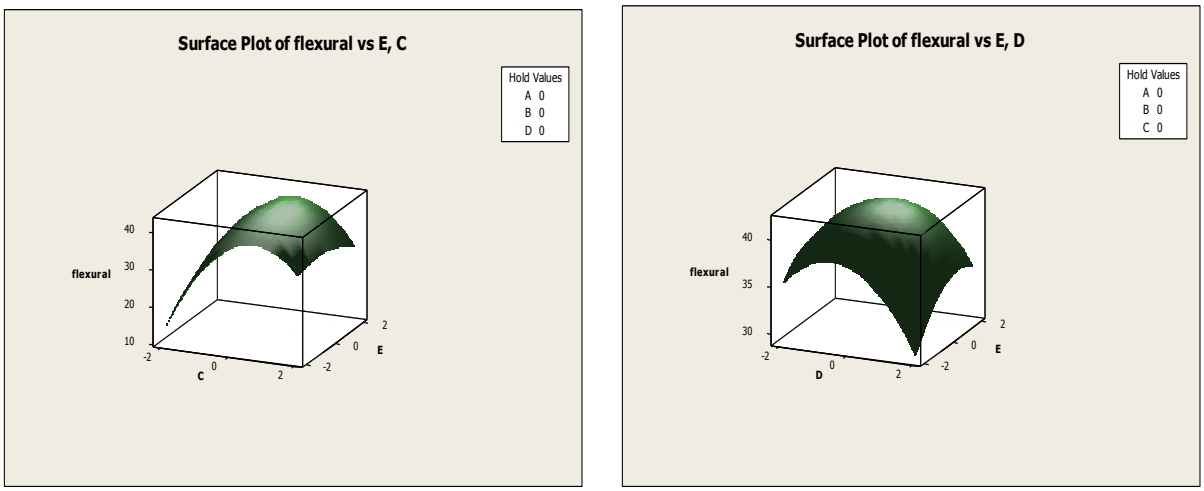

Figure 5.9 Surface plots of flexural test

Flexural strength response surface shows that flexural strength monotonously increases with increase in layer thickness (A) .The reason may be that for flexural strength measurement load is applied perpendicular to length of specimen. Therefore thicker part will show more strength as compared to thinner part. Hence, if part is made with thicker layer then each individual layer will show more resistance against the failure as compared to part of same thickness made with thinner layer.

Flexural strength of the material is first increasing with respect to sample orientation (B) and after certain level it gets decrease, this is may be due to the stepped effect, in this layer deposited over another layer so due the sample orientation there may be some portion is vacant this lead to the weak strength of material.

At lower raster angle (C) not only the length of individual raster is more but their inclination along the length of specimen is also more as result strength will be more. Combine effect of long raster and thick layer is responsible for monotonous increase in strength at small raster angle value with increase in layer thickness. But long rasters have more distortion as compare to short rasters as a result strength will increase on increasing the raster angle.

Higher width (D) reducing the number of rasters due to which the rasters are not able to give much resistance for the applied load. Higher raster not only reduces the number of rasters but also inputting more heat into the system as a result strength will decrease.

Flexural strength is increased with increasing the air gap (E), this is due to that, at min. air gap two raster will be very close and this decreases the heat dissipation and increase the chance of residual stress accumulation. This lead to reduce the strength at low level of air gap.

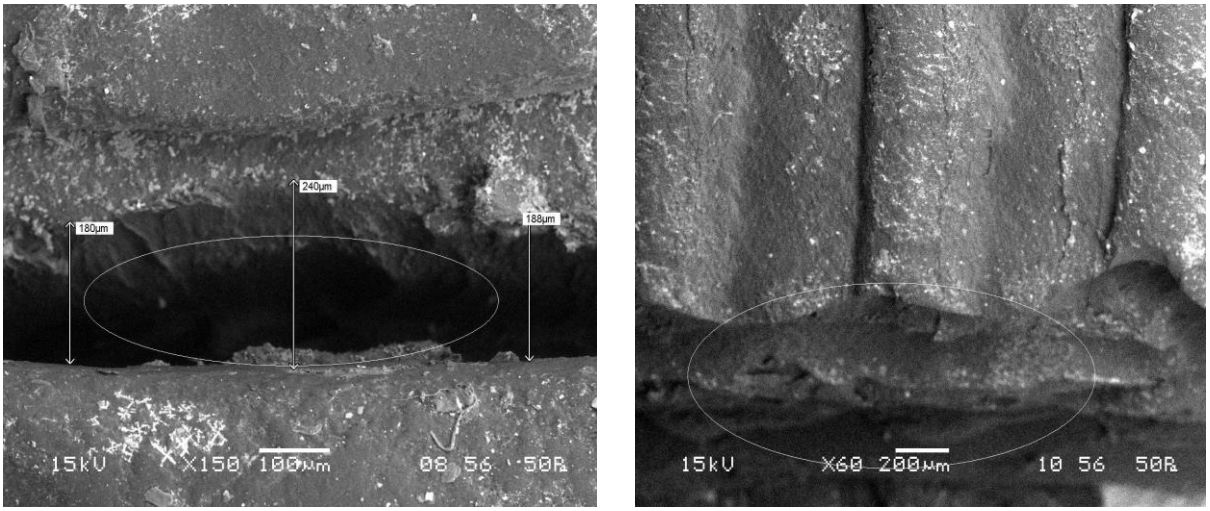

(c) Crack formation in flexural specimen (d) specimen after cracking

Figure 5.10 SEM image of crack surface of flexural specimen

SEM image of 3-point bending test specimen is shown in Image (c) and (d) respectively. Image (c) shows the crack occurred after bending test, in fig we can see that the cracking length is max, where max. Load is applied .and in Image (d) the horizontal position of the cracked specimen is shown, although ABS P400 (acrylonitrile-butadine-styrene) is a brittle material so we can see in the Image (d) no or negligible elongation took place.

5.3.5 Analysis of experiment for impact test:

Table 5.7 Estimated regression coefficients for impact test

Term	Coef.	SE Coef.	T	P
Constant	14.9724	0.15296	97.884	0.000
A	0.2004	0.07828	2.560	0.027
B	0.1971	0.07828	2.518	0.029
C	-0.1779	0.07828	-2.273	0.044
D	0.0588	0.07828	0.751	0.469
E	0.6429	0.07828	8.213	0.000
A*A	-0.7549	0.07081	-10.661	0.000
B*B	-0.8224	0.07081	-11.614	0.000
C*C	-0.4974	0.07081	-7.025	0.000
D*D	-0.7349	0.07081	-10.379	0.000
E*E	-0.4849	0.07081	-6.848	0.000
A*B	0.1444	0.09587	1.506	0.160
A*C	-0.6556	0.09587	-6.838	0.000
A*D	-0.0606	0.09587	-0.632	0.540
A*E	0.0506	0.09587	0.528	0.608
B*C	0.1569	0.09587	1.636	0.130
B*D	-0.3481	0.09587	-3.631	0.004
B*E	-0.1869	0.09587	-1.949	0.077
C*D	-0.0106	0.09587	-0.111	0.914
C*E	-0.1369	0.09587	-1.428	0.181
D*E	-0.1044	0.09587	-1.089	0.300

S = 0.3835 R^2 = 97.9% R^2 (adj) =94.0%

With the above analysis we found factors A, B, C, E and interaction A*A, B*B, C*C, D*D, E*E, A*C, B*D.

The coefficient of determination (R^2) which indicates the goodness of fit for the model so the value of R^2 =97.9% which indicate the high significance of the model.

With the above analysis we found the following regression equation:-

Is = 14.9724 + 0.2004A + 0.1971B – 0.1779C + 0.6429E – 0.7549(A*A) – 0.8224(B*B) - 0.4974 (C*C) – 0.7349 (D*D) - 0.4849 (E*E) – 0.6556 (A*C) – 0.3481(B*D) .

Table 5.8 Analysis of variance for impact test

Source	DF	Tensile strength			
		SS	MS	F	p
Regression	20	74.2303	3.7115	25.24	0.000
Linear	5	12.6590	2.5318	17.22	0.000
Square	5	50.8931	10.1786	69.21	0.000
Interaction	10	10.6783	1.0678	7.26	0.001
Residual	11	1.6177	0.1471		
Lack of fit	6	1.2494	0.2082	2.83	0.137
Pure error	5	0.3683	0.0737		
Total	31	75.8480			

DF =degree of freedom SS = sum of square MS = mean sum of square

In the above table we can see P value of all the term is less than 0.05, so these all term are significant, and non significance lack of fit is desired in this case value of LOF is 0.077 which is more than 0.05 and non significant.

5.3.6 Response analysis for impact test:

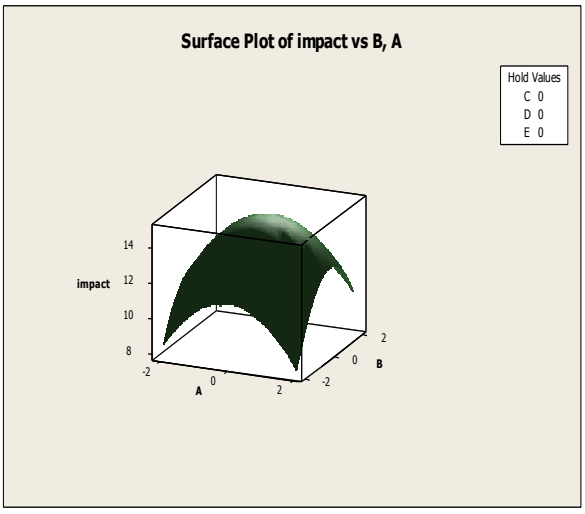

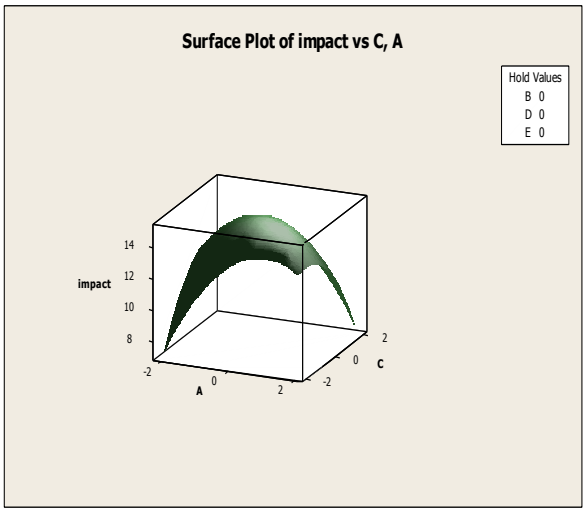

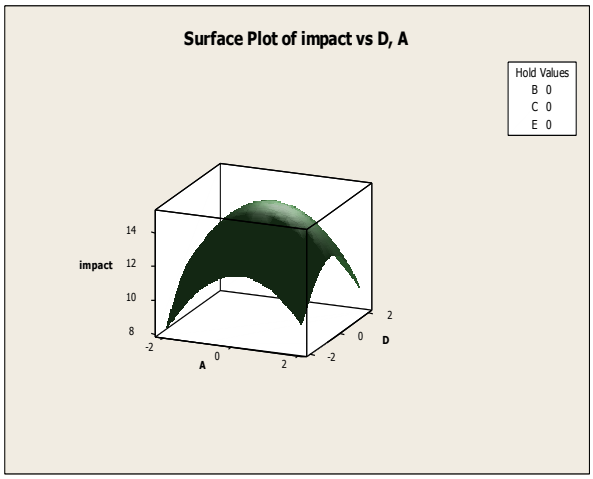
Surface Plot of impact vs D, A
Hold Values
B 0
C 0
E 0
impact
A
D

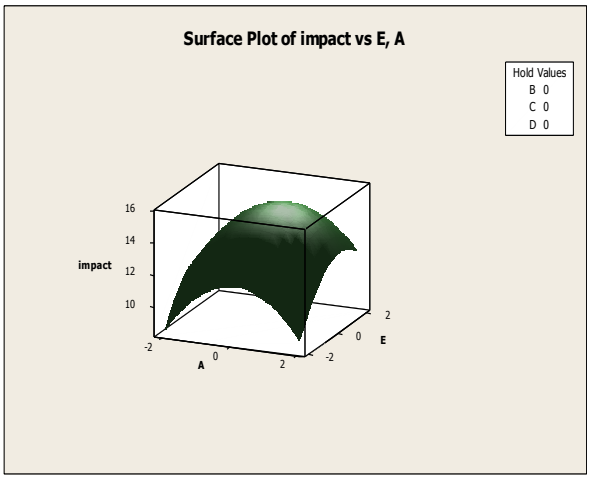
Surface Plot of impact vs E, A
Hold Values
B 0
C 0
D 0
impact
A
E

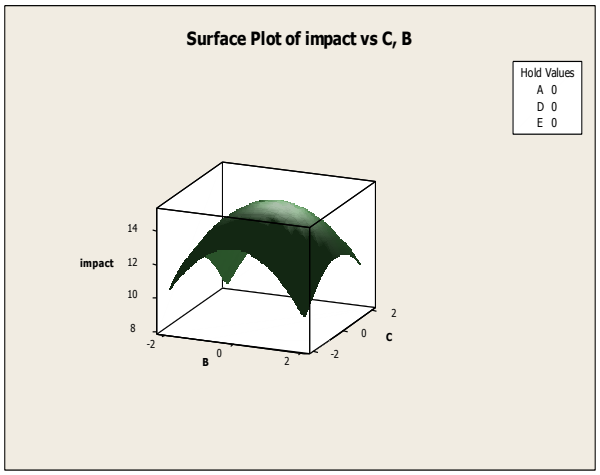
Surface Plot of impact vs C, B
Hold Values
A 0
D 0
E 0
impact
B
C

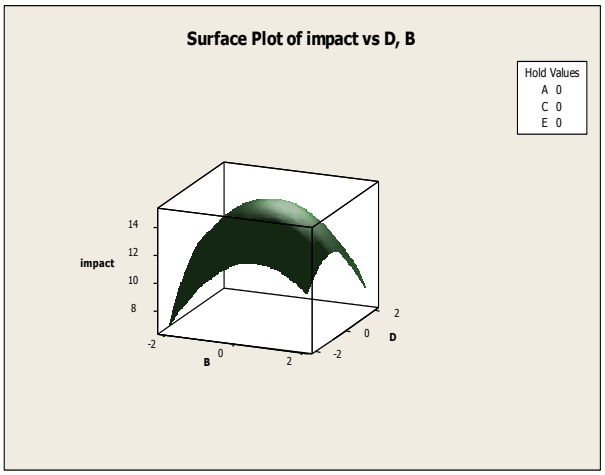
Surface Plot of impact vs D, B
Hold Values
A 0
C 0
E 0
impact
B
D

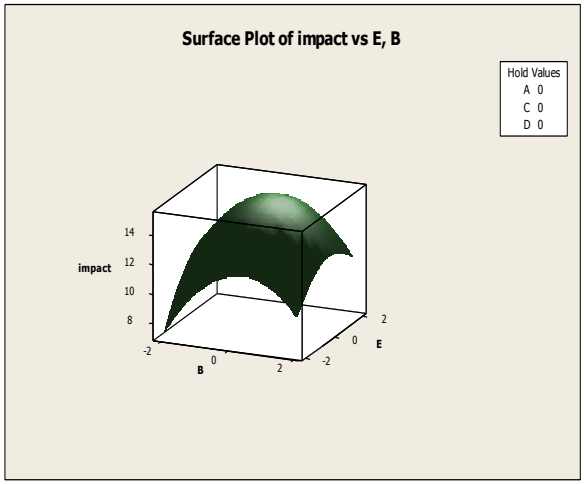
Surface Plot of impact vs E, B
Hold Values
A 0
C 0
D 0
impact
B
E

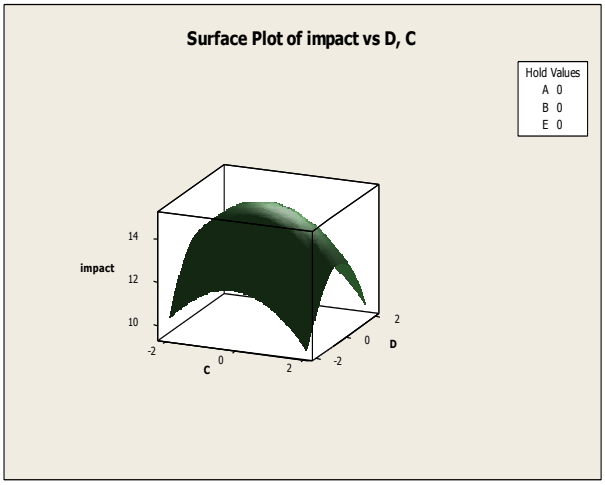
Surface Plot of impact vs D, C
Hold Values
A 0
B 0
E 0
impact
C
D

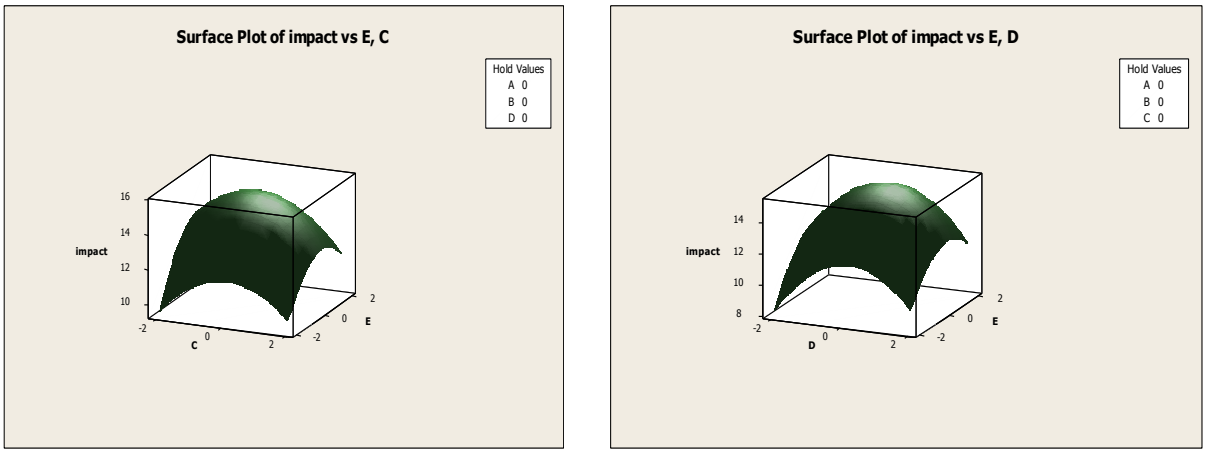

Figure 5.11 Surface plots of impact test

With the above graphs we can see that behavior of all the factors are similar and up to level 0 of the factors strength is increasing and after that level its decreasing, this is may be due to the reason which we have discussed in tensile strength analysis and flexural strength analysis.

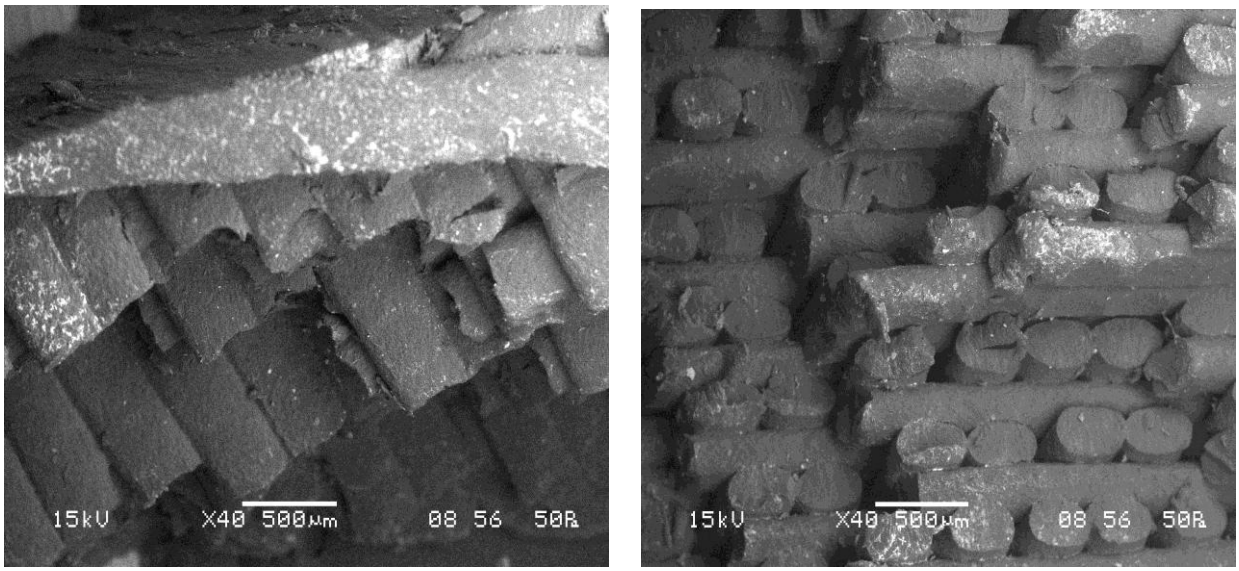

(e) Horizontal position of broke specimen (f) vertical position of broke specimen

Figure 5.12 SEM image of broke impact test specimen

In above SEM image two image shown (e) and (f) respectively for horizontal and vertical position of the impact specimen. Image (e) shows the behavior of material after breaking. In this test material directly break from the notch portion with the help of pendulum. And it is the ABS P400 (acrylonitrile-butadine-styrene) material which behaves as a brittle material, this directly break and no elongation takes place, this we can see in image (e) and (d) that the material broke at different place due to sudden impact load, but no change or elongation in any dimension of the shape took place.

With the above three analysis we see that tensile strength is higher in experiment no. 2, flexural strength is higher in experiment no. 31, and impact strength is higher in experiment no. 28. And factors and interactions which are affecting the strength are different in three cases. So to optimize all the response simultaneously by converting multiple response into single response Gery-taguchi method is used.

5.4 Optimization of process parameters

Above discussion shows that FDM process involves large number of conflicting factors and complex part building phenomena making it difficult to predict the output characteristics based on simple analysis of factor variation. Hence, to determine the optimal setting of process parameters that will maximize the tensile strength, flexural strength and impact strength respectively, desirability function (DF) given by Equation (5.1) is used

$$DF = \left(\prod_{i=1}^{n} d_i^{w_i} \right)^{1/\sum_{i=1}^{n} w_i} \quad \text{.....(5.1)}$$

where d_i is the desirability defined for the i^{th} targeted output. For a goal to find a maximum, d_i is calculated as shown in Equation (5.2).

$$
\begin{aligned}
d_i &= 0 && \text{if} && Y_i \le \text{low}_i \\
d_i &= \left[\frac{Y_i - \text{low}_i}{\text{High}_i - \text{low}_i}\right] && \text{if} && \text{Low}_i < Y_i < \text{High}_i \\
d_i &= 1 && \text{if} && Y_i \ge \text{High}_i
\end{aligned}
\qquad \text{.....(5.2)}
$$

where Y_i is the found value of the i^{th} output during optimization process, and the low_i, $High_i$ are the minimum and maximum values respectively of the experimental data for the i^{th} output. Since all the strengths are equally important therefore value of weight w_i is taken as 1.Optimum factor levels that will maximize the desirability function are calculated and are given in Table (5.10) for respective strength together with its predicted value.

Table 5.9 Optimum factor and predicted response for individuals strength

Response	Goal	Low	High	w_i	Factor level (Coded units)	Predicted response	DF
Tensile strength	Maximum	11.04	17.76	1	A=2; B=-2; C=-2; D= -2; E=-2	19.43	1.0000
Flexural strength	Maximum	19.2	42.3	1	A=0; B=0; C=0; D=0; E=0.4968	41.88	0.98185
Impact strength	Maximum	10.4	15.5	1	A=0; B=0; C=0; D=0; E=0.6835	15.1853	0.93829

CHAPTER 6

GREY – BASED TAGUCHI METHOD

6. Grey-based taguchi method

6 .1 Introduction :

Taguchi's philosophy, developed by Dr. Genichi Taguchi, is an efficient tool for the design of high quality manufacturing system [30]. It is a method based on Orthogonal Array experiments which provides much-reduced variance for the experiment resulting optimal setting of process control parameters. Orthogonal Array provides a set of well-balanced experiments with less number of experimental runs. In order to evaluate the optimal parameter setting, Taguchi method uses a statistical measure of performance called signal-to-noise ratio that takes both the mean and the variability into account. The S/N ratio is the ratio of the mean (signal) to the standard deviation (noise). The ratio depends on the quality characteristics of the product/process to be optimized. The standard S/N ratios generally used are Nominal-is-Best (NB), lower-the-better (LB) and Higher-the-Better (HB). The optimal setting is the parametric combination, which has the highest S/N ratio. However, traditional Taguchi method cannot solve multi-objective optimization problem. This can be achieved by grey based Taguchi method. In grey relational analysis, experimental data i.e. measured features of quality characteristics of the product are first normalized ranging from zero to one. This process is known as grey relational generation. Next, based on normalized experimental data, grey relational coefficient is calculated to represent the correlation between the desired and actual experimental data. Then, overall grey relational grade is determined by averaging the grey relational coefficient corresponding to selected responses. The overall performance characteristic of the multiple response process

depends on the calculated overall grey relational grade. This approach converts a multiple-response process optimization problem into a single response optimization situation with the objective function is overall grey relational grade. Using grey-Taguchi method, the optimal parametric combination is then evaluated by maximizing the S/N ratio of the overall grey relational grade.

6.2 Grey-relational analysis:

Data preprocessing:

Grey data processing must be performed before Grey correlation coefficients can be calculated. A series of various units must be transformed to be dimensionless. Usually, each series is normalized by dividing the data in the original series by their average. Let the original reference sequence and sequence for comparison be represented as xo(k) and xi (k), i =1, 2, ...,m; k =1, 2, ..., n, respectively, where m is the total number of experiment to be considered, and n is the total number of observation data. Data preprocessing converts the original sequence to a comparable sequence [30]. Several methodologies of preprocessing data can be used in Grey relation analysis, depending on the characteristics of the original sequence. If the target value of the original sequence is "the-larger-the-better", then the original sequence is normalized as follows:

$$x_i^*(k) = \frac{x_i^*(k) - \min x_i^0(k)}{\max x_i^0(k) - \min x_i^0(k)}, \tag{1}$$

If the expectancy is smaller- the –better, then the original sequence should be normalized as follow.

$$x_i^*(k) = \frac{\max x_i^0(k) - x_i^0(k)}{\max x_i^0(k) - \min x_i^0(k)}. \tag{2}$$

However, there is a definite target value to be achieved; the original sequence will be normalized in the form.

$$x_i^*(k) = 1 - \frac{|x_i^0(k) - x^0|}{\max x_i^0(k) - x^0} \tag{3}$$

or the original sequence can be simply normalized by the most basic methodology, i.e. let the values of original sequence be divided by the first value of sequence:

$$x_i^*(k) = \frac{x_i^0(k)}{x_i^0(1)}, \tag{4}$$

where $x^*_i(k)$ is the value after the grey relational generation (data pre-processing), max x^0_i (k) is the largest value of x^0_i (k), min x^0_i (k) is the smallest value of x^0_i (k) and x^0 is the desired value.

Grey relational coefficient and grey relational grade:

Following data pre-processing, a grey relational coefficient is calculated to express the relationship between the ideal and actual normalized experimental results. The grey relational coefficient can be expressed as follows:

$$\xi_i(k) = \frac{\Delta_{\min} + \zeta \cdot \Delta_{\max}}{\Delta_{0i}(k) + \zeta \cdot \Delta_{\max}}, \tag{5}$$

where $\Delta^0_i(k)$is the deviation sequence of the reference sequence $x^*_0(k)$ and the comparability sequence $x^*_i(k)$, namely

$$\Delta_{0i}(k) = \|x_0^*(k) - x_i^*(k)\|,$$

$$\Delta_{\max} = \max_{\forall j \in i} \max_{\forall k} \|x_0^*(k) - x_j^*(k)\|,$$

$$\Delta_{\min} = \min_{\forall j \in i} \min_{\forall k} \|x_0^*(k) - x_j^*(k)\|.$$

ξ is distinguishing or identification coefficient: ξ ε [0,1]. ξ =0.5 is generally used.

After obtaining the grey relational coefficient, we normally take the average of the grey relational coefficient as the grey relational grade. The grey relational grade is defined as follows:

$$\gamma_i = \frac{1}{n} \sum_{k=1}^{n} \xi_i(k). \tag{6}$$

However, since in real application the effect of each factor on the system is not exactly same. Eq. (6) can be modified as follow:

$$\gamma_i = \sum_{k=1}^{n} w_k \cdot \xi_i(k) \qquad \sum_{k=1}^{n} w_k = 1, \tag{7}$$

Where w_k represents the normalized weighting value of factor k. Given the same weights, Eqs. (6) and (7) are equal. In the grey relational analysis, the grey relational grade is used to show the relationship among the sequences. If the two sequences are identical, then the value of grey relational grade is equal to 1. The grey relational grade also indicates the degree of influence that the comparability sequence could exert over the reference sequence. There- fore, if a particular comparability sequence is more important than the other comparability sequences to the reference sequence, then the grey relational grade for that comparability sequence and reference sequence will be higher than other grey relational grades [31] .

In this analysis we are considering three responses tensile strength, flexural strength, impact strength, these response should be high, so we normalizing the data according to larger -the-better(LB).

Table 6.1 . Normalization of the data (larger-the-better) ($x^*_i(k)$)

Experiment no.	Tensile strength	Flexural strength	Impact strength
Ideal condition	1.00000	1.00000	1.00000
1	0.07440	0.54113	0.27451
2	1.00000	0.52814	0.17647
3	0.00000	0.25108	0.01961
4	0.39435	0.31602	0.70588
5	0.18601	0.54978	0.08824
6	0.19494	0.98701	0.18627
7	0.01637	0.55844	0.48039

8	0.18601	0.84848	0.23529
9	0.84673	0.47186	0.07647
10	0.76339	0.53680	0.66667
11	0.00000	0.45455	0.09804
12	0.12202	0.00000	0.29412
13	0.28274	0.54545	0.47059
14	0.67857	0.54978	0.00000
15	0.00149	0.71429	0.25490
16	0.78423	0.64069	0.19020
17	0.01488	0.88745	0.21569
18	0.75298	0.86147	0.34118
19	0.81994	0.55411	0.07843
20	0.00000	0.21645	0.37255
21	0.67857	0.09091	0.58824
22	0.18750	0.64935	0.37255
23	0.18155	0.79221	0.19608
24	0.79762	0.72727	0.39216
25	0.43750	0.88745	0.21569
26	0.20238	0.89177	0.76471
27	0.61905	0.99567	0.88235
28	0.78274	0.90476	1.00000
29	0.72321	0.96970	0.84314
30	0.79762	0.94805	0.90196
31	0.66369	1.00000	0.92157
32	0.72321	0.97835	0.88235

Table 6.2 The deviation sequence ($\Delta_{o,i}(k)$)

Experiment no.	Tensile strength, $\Delta o,i(1)$	Flexural strength, $\Delta o,i(2)$	Impact strength, $\Delta o,i(3)$
1	0.92560	0.45887	0.72549
2	0.00000	0.47186	0.82353
3	1.00000	0.74892	0.98039
4	0.60565	0.68398	0.29412
5	0.81399	0.45022	0.91176
6	0.80506	0.01299	0.81373

7	0.98363	0.44156	0.51961
8	0.81399	0.15152	0.76471
9	0.15327	0.52814	0.92353
10	0.23661	0.46320	0.33333
11	1.00000	0.54545	0.90196
12	0.87798	1.00000	0.70588
13	0.71726	0.45455	0.52941
14	0.32143	0.45022	1.00000
15	0.99851	0.28571	0.74510
16	0.21577	0.35931	0.80980
17	0.98512	0.11255	0.78431
18	0.24702	0.13853	0.65882
19	0.18006	0.44589	0.92157
20	1.00000	0.78355	0.62745
21	0.32143	0.90909	0.41176
22	0.81250	0.35065	0.62745
23	0.81845	0.20779	0.80392
24	0.20238	0.27273	0.60784
25	0.56250	0.11255	0.78431
26	0.79762	0.10823	0.23529
27	0.38095	0.00433	0.11765
28	0.21726	0.09524	0.00000
29	0.27679	0.03030	0.15686
30	0.20238	0.05195	0.09804
31	0.33631	0.00000	0.07843
32	0.27679	0.02165	0.11765

Table 6.3 Calculation of grey relational coefficients($\xi_i(k)$)

Experimental no.	Tensile strength (MPa)	Flexural strength(MPa)	Impact strength(joules)
1	0.35073	0.52145	0.40800
2	1.00000	0.51448	0.37778
3	0.33333	0.40035	0.33775
4	0.45222	0.42230	0.62963
5	0.38052	0.52619	0.35417
6	0.38312	0.97468	0.38000
7	0.33701	0.53103	0.49038
8	0.38052	0.76744	0.39535

9	0.76538	0.48632	0.35124
10	0.67879	0.51910	0.60000
11	0.33333	0.47826	0.35664
12	0.36285	0.33333	0.41463
13	0.41076	0.52381	0.48572
14	0.60869	0.52619	0.33333
15	0.33366	0.63637	0.40157
16	0.69855	0.58186	0.38174
17	0.33667	0.81626	0.38931
18	0.66933	0.78305	0.43147
19	0.73523	0.52860	0.35172
20	0.33333	0.38954	0.44348
21	0.60869	0.35484	0.54839
22	0.38095	0.58779	0.44348
23	0.37923	0.70642	0.38346
24	0.71187	0.64706	0.45133
25	0.47059	0.81626	0.38931
26	0.38532	0.82206	0.68000
27	0.56757	0.99141	0.80952
28	0.69710	0.84000	1.00000
29	0.64367	0.94286	0.76120
30	0.71187	0.90588	0.83606
31	0.59786	1.00000	0.86441
32	0.64367	0.95850	0.80952

Table 6.4 Grey- relational grade (γ_i)

Ex. No.	γ_i
1	0.42672
2	0.63075
3	0.35714
4	0.50138
5	0.42029
6	0.57926
7	0.45280
8	0.51443
9	0.53431
10	0.59929
11	0.38941

12	0.37027
13	0.47343
14	0.48940
15	0.45720
16	0.55405
17	0.51408
18	0.62795
19	0.53851
20	0.38878
21	0.50397
22	0.47074
23	0.48970
24	0.60342
25	0.55872
26	0.62912
27	0.78950
28	0.84570
29	0.78257
30	0.81793
31	0.82075
32	0.80389

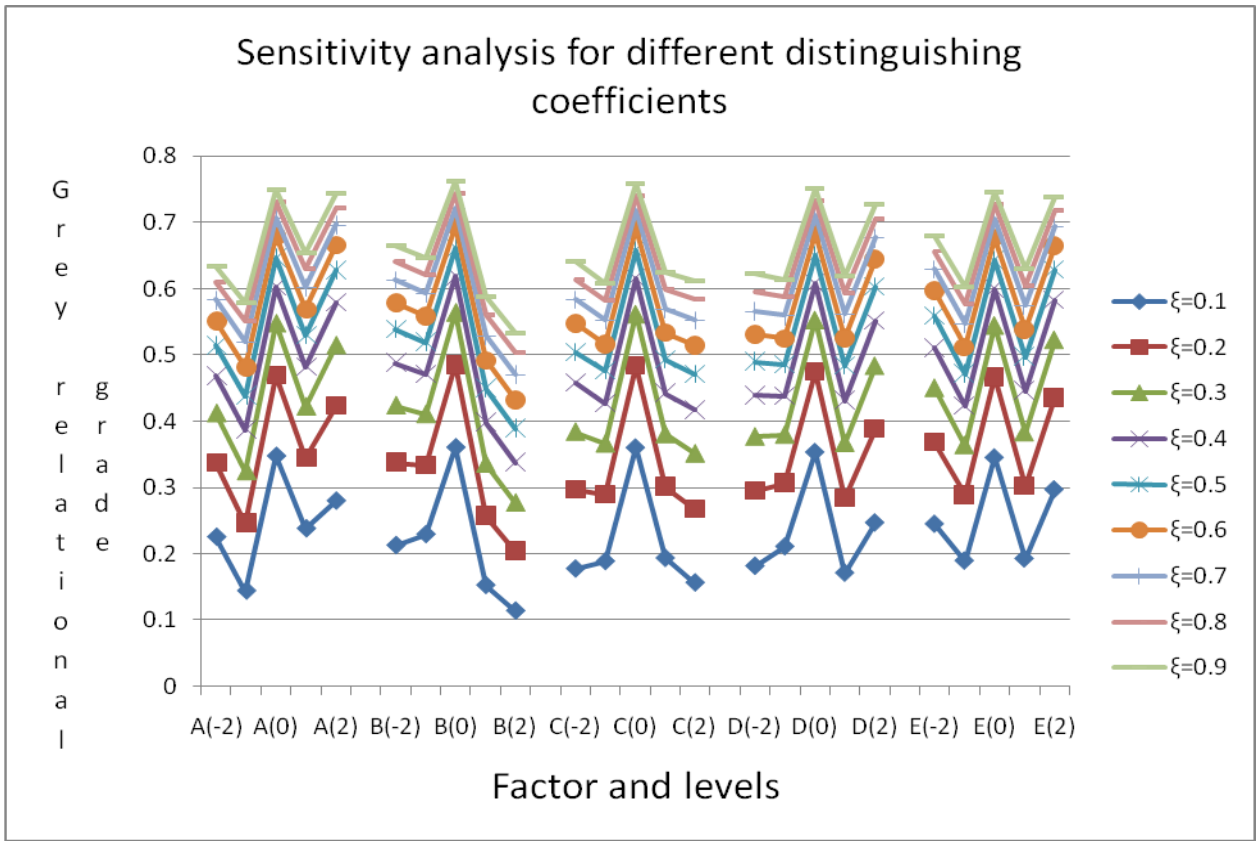

Figure 6.1. Sensitivity analysis for different distinguishing coefficients(ξ)

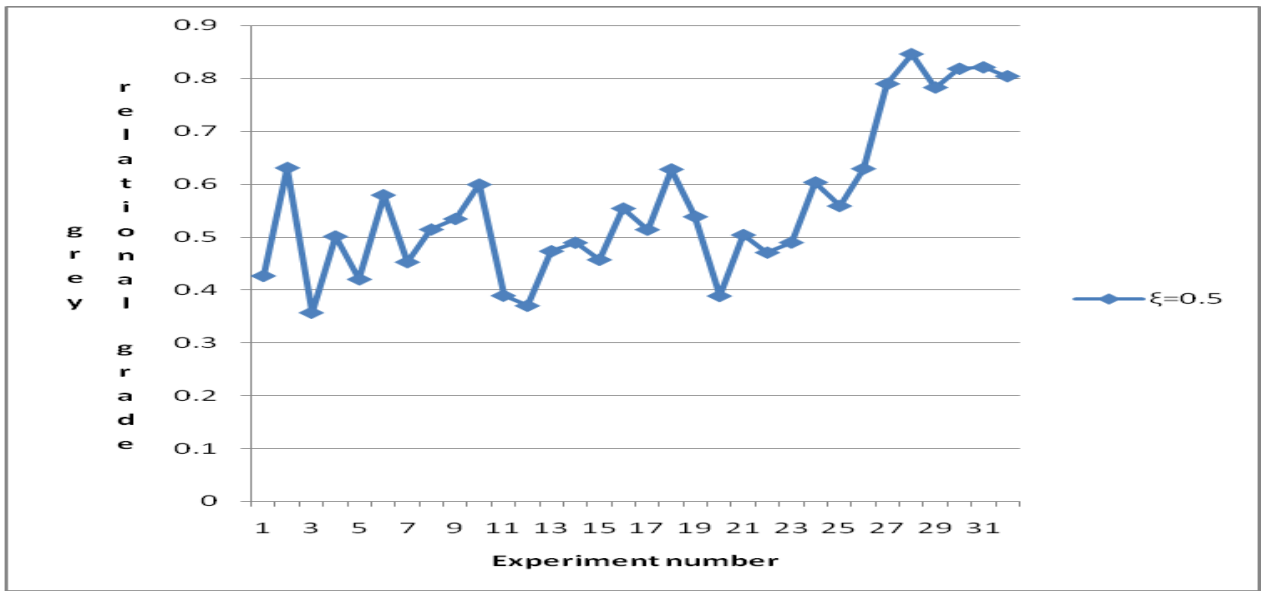

Figure 6.2 . Grey relational grade variation with number of experiment(ξ=0.5)

The purpose of distinguish coefficient is to expand or compress the range of the grey relational coefficient. The distinguishing coefficient can be selected by decision maker judgement, and different distinguishing coefficients usually provide different results in GRA. Sensitivity analysis for different distinguishing coefficients (Figure 19) shows that impact of their variation on grey relation coefficient is very small. They all led to the same optimum factor levels. In this case distinguishing coefficient is taken as 0.5.

Table 6.5 Response surface analysis for grey relational grade

S.N.	A	B	C	D	E	Grey-relational grade
1	-1	-1	-1	-1	1	0.42672
2	1	-1	-1	-1	-1	0.63075
3	-1	1	-1	-1	-1	0.35714
4	1	1	-1	-1	1	0.50138
5	-1	-1	1	-1	-1	0.42029
6	1	-1	1	-1	1	0.57926
7	-1	1	1	-1	1	0.45280
8	1	1	1	-1	-1	0.51443
9	-1	-1	-1	1	-1	0.53431
10	1	-1	-1	1	1	0.59929
11	-1	1	-1	1	1	0.38941
12	1	1	-1	1	-1	0.37027
13	-1	-1	1	1	1	0.47343
14	1	-1	1	1	-1	0.48940
15	-1	1	1	1	-1	0.45720
16	1	1	1	1	1	0.55405
17	-2	0	0	0	0	0.51408
18	2	0	0	0	0	0.62795
19	0	-2	0	0	0	0.53851
20	0	2	0	0	0	0.38878
21	0	0	-2	0	0	0.50397
22	0	0	2	0	0	0.47074
23	0	0	0	-2	0	0.48970
24	0	0	0	2	0	0.60342
25	0	0	0	0	-2	0.55872
26	0	0	0	0	2	0.62912

27	0	0	0	0	0	0.78950
28	0	0	0	0	0	0.84570
29	0	0	0	0	0	0.78257
30	0	0	0	0	0	0.81793
31	0	0	0	0	0	0.82075
32	0	0	0	0	0	0.80389

Table 6.6 Estimated Regression coefficients for grey relational grade

Term	Coef.	SE Coef.	T	P
Constant	0.806193	0.013399	60.170	0.000
A	0.039803	0.006857	5.805	0.000
B	-0.035677	0.006857	-5.203	0.000
C	0.002714	0.006857	0.396	0.700
D	0.008833	0.006857	1.288	0.224
E	0.014307	0.006857	2.087	0.061
A*A	-0.055893	0.006206	-9.012	0.000
B*B	-0.082735	0.006206	-13.339	0.000
C*C	-0.076808	0.006206	-12.384	0.000
D*D	-0.062007	0.006206	-9.997	0.000
E*E	-0.050166	0.006206	-8.088	0.000
A*B	-0.010024	0.008398	-1.194	0.258
A*C	-0.003793	0.008398	-0.452	0.660
A*D	-0.025638	0.008398	-3.053	0.011
A*E	0.015982	0.008398	1.903	0.084
B*C	0.036812	0.008398	4.383	0.001
B*D	-0.005890	0.008398	-0.701	0.498
B*E	0.012165	0.008398	1.449	0.175
C*D	0.001875	0.008398	0.223	0.827
C*E	0.009618	0.008398	1.145	0.276
D*E	0.007965	0.008398	0.948	0.363

S= 0.03359 **R-sq= 98.0%** **R-sq (adj) = 94.4%**

With the above analysis we found while considering all the response simultaneously only factor (A), and (B), and interaction term A*A, B*B, C*C, D*D, E*E, A*D, B*C.

The coefficient of determination (R^2) which indicates the percentage of total variation in the response explained by the terms in the model is 98%.

With the above analysis we found the following regression equation:-

Os =0.806193+0.039803A – 0.035677B -0.055893(A*A) – 0.082735(B*B) – 0.076808(C*C) - 0.062007 (D*D) - 0.050166(E*E) – 0.025638(A*D)+0.036812(B*C) .

Table 6.7 ANOVA analysis for grey relational grade

Source	DF	Tensile strength			
		SS	MS	F	p
Regression	20	0.615837	0.030792	27.29	0.000
Linear	5	0.075534	0.015107	13.39	0.000
Square	5	0.496706	0.099341	88.03	0.000
Interaction	10	0.043597	0.004360	3.86	0.018
Residual	11	0.012413	0.001128		
Lack of fit	6	0.009750	0.001625	3.05	0.121
Pure error	5	0.002663	0.000533		
Total	31	0.628250			

6.3 Response Optimization of GRG and optimal parameter setting:

With the help of response optimizer we have found the optimal parameter setting for all three responses:

	Goal	Lower	Target	Upper	Weight	Importance
response	Maximum	0.35714	1	1	1	1

Predicted GRG Responses = 0.80619
desirability = 0.80619

For the above predicted response the optimal parameter setting is

Parameter	value	Units
Layer thickness	0.190	(mm)
Sample orientation	30	(degree)
Raster angle	30	(degree)
Raster width	0.4464	(mm)
Air gap	0.004	(mm)

Table 6.8 Comparison of parameter setting individual and simultaneous optimization (Uncoded Value)

Parameter	Individual optimization			Simultaneous optimization
	Tensile strength	Flexural strength	Impact strength	
A (mm)	0.254	0.190	0.190	0.190
B (degree)	0	30	30	30
C (degree)	0	30	30	30
D (mm)	0.4064	0.4464	0.4464	0.4464
E (mm)	0	0.004993	0.005367	0.004

CHAPTER 7

RESULT, CONCLUSION AND FUTURE SCOPE

7. Results, conclusions and future scope

7.1 Results and discussions:

The tensile strength data of ABS sample with different level of process parameter are shown in table (2). The ultimate strength were the highest (17.76 MPa) for the layer thickness 0.222 mm, sample orientation 15^o , raster angle 15^o , raster width 0.4264 mm, and air gap 0.002 mm combination set and the lower strength (11.04 MPa) for layer thickness 0.158 mm, sample orientation 45^o, raster angle 15^o , raster width 0.4264 mm, and air gap 0.002 mm, the lower strength in the solid model could have been caused by residual stress from the volumetric shrinkage , weak interlayer bonding, or interlayer porosity. Examination of the fracture surfaces revealed fracture paths that were controlled by either weak interlayer bonding or interlayer porosity. Weak interlayer bonding probably was a result of residual stresses caused by volumetric shrinkage of the polymer layers during solidification from the melt. Weak interlayer bonding could also be caused by the low molecular diffusion and low cross-linking between the polymer layers during deposition from the melt. In addition, the interlayer porosity reduced the load-bearing area across the layers and hence provided an easy fracture path. The percent elongation of the tensile specimens was <2%, and the ABS material failed in a semi-brittle manner. Because the ABS elongation was so low.

The 3-point bending test data of ABS sample shown in table (2).the flexural strength are greater than the tensile strengths because the modulus of rupture measure the maximum strength at the outer fiber of the beam. This is expected because during bending, the sample is subjected to both compressive and tensile load in this test flexural strength is highest (42.3 MPa) for the layer thickness 0.190 mm, sample orientation 30^o , raster angle 30^o, raster width 0.4464 mm, and air gap were 0.004 mm. and min. flexural strength (19.20 MPa) for layer thickness 0.222 mm,

sample orientation 45^{o}, raster angle 15^{o} , raster width 0.4664 mm, and air gap 0.002 mm. again as in the tensile testing, this low flexural strength is due to rapid prototyping sample having weak interlayer bonding or interlayer porosity.

During impact testing, the material is subjected to quick, intense blow by a hammer pendulum. The impact test measures the energy absorption or the toughness of the material. The V-notched specimen evaluates the materials resistance to crack propagation. In this test we found ultimate impact strength (15.50 joule) for the parametric combination of layer thickness 0.190 mm, sample orientation 30^{o}, raster angle at 30^{o}, raster width 0.4464 mm, and air gap 0.004 mm. and min. impact strength (10.4 joule) for the parametric combination of layer thickness 0.222 mm, sample orientation 15^{o}, raster angle 45^{o}, raster width 0.4664 mm, and air gap 0.002 mm. in FDM, heating and rapid cooling cycles of the material result in non-uniform temperature gradients. This cause stresses to build up leading to distortion, dimensional inaccuracy and inner layer cracking or de-lamination. The reasons attributed to non uniform heating and cooling cycles are explained as follows:

(1) In FDM, heat is dissipated by conduction and forced convection and the reduction in temperature caused by these processes forces the material to quickly solidify onto the surrounding filaments. Bonding between the filaments is caused by local re-melting of previously solidified material and diffusion. This results in uneven heating and cooling of material and develops non uniform temperature gradients. As a result, uniform stress will not be developed in the deposited material and it may not regain its original dimension completely.

(2) Speed at which nozzle is depositing the material may alter the heating and cooling cycle and results in different degree of thermal gradient and thus also affects the part accuracy.

At lower slice thickness, nozzle deposition speed is slower as compared to higher slice thickness. Also during deposition, nozzle stops depositing material in random manner (in between depositing a layer and after completely depositing a layer) and return to service location for tip cleaning. While depositing the material at the turns near the boundary of part, nozzle speed has to be decreased and then increase to uniform speed . If deposition path length is small, this will result in non uniform stress to build up especially near the part boundary.

(3) The pattern used to deposit a material in a layer has a significant effect on the resulting stresses and deformation. Higher stresses will be found along the long axis of deposition line. Therefore, short raster length is preferred along the long axis of part to reduce the stresses.

(4) Stress accumulation also increase with layer thickness and road width. But the thick layer also means fewer layers, which may reduce the number of heating and cooling cycles. Also, a smaller road width will input less heat into the system within the specified period of time but requires more loops to fill a certain area. More loops means more time required for deposition of single layer and more non uniform nozzle speed. This will keep the deposited material above its desired temperature for regaining its original shape and in the mean time new material will be deposited and contraction of previously deposited material will be constrained

Hence, with the response surface analysis we have seen that tensile strength, flexural strength, and impact strength, are higher at different parametric combination, optimization of all three responses is impossible. So grey Taguchi method is used to convert these multiple response into a single response, and with the help of response optimizer we found out the optimal parameter setting to maximize all three responses.

7.2 Conclusion:

Effect of five process parameters layer thickness, sample orientation, raster angle, raster width and air gap are studied on three responses viz., tensile strength, flexural strength and impact strength of test specimen. Experiments were conducted using centre composite design (CCD). Empirical relations between each response and process parameters were determined and their validity is proved using analysis of variance (ANOVA) and the normal probability plot of residues. Response surface plots of respective strength shows that parameter effect are dependent on each other and their optimal setting depends upon the level selected for other parameters. The main reason attributed for weak strength is the distortion within the layer or between the layers. To get the optimal level concept of simultaneous optimization of three responses desirability function is used for maximizing the all the responses and found out the optimal parameter setting.

7.3 Future scope:

The response surface methodology is a robust process for optimization of the single response as well as multiple responses. In present work, optimization of three FDM responses is considered are tensile, flexural, and impact strength. Due to time constraints, we optimized only three responses, although compression test, fatigue test, wear test, hardness test, may be carried out in future. Response surface methodology can be used as an analysis tool in any process when parameters affecting the responses are identified through experimental and theoretical validation.

BIBLIOGRAPHY

Bibliography

1. Wiedemann, B. Jantzen (1999). Strategies and applications for rapid product and process development in Daimler-Benz AG, Computers in industries, 39(1):11–25
2. Upcraft Steve and Fletcher Richard (2003). The Rapid prototyping technologies, Rapid prototyping journal,23(4):318-330
3. Mansour S. and Hauge R (2003). Impact of rapid manufacturing on design for manufacturing on design for manufacture for injection moulding, Proceedings of the institution of mechanical enginers, Part B, Journal of engineering manufacture, 217(4): 453-461
4. Ahn Sung Hoon, Montero Michael, Odell Dan, Roundy Shad, Wright Paul K. (2002). Anisotropic material properties of fused deposition modelling ABS, Rapid prototyping journal, 8 (4): 248-257
5. Es. Said Os, Foyos J, Noorani R, Mandelson M, Marloth R, Pregger BA (2000). Effect of layer orientation on mechanical properties of rapid prototyped samples, Materials and manufacturing process,15 (1):107-122.
6. Lee C.S., Kim S.G., Kim H.J., Ahn S.H (2007), Measurement of anisotropic compressive strength of rapid prototyping parts, Journal of materials processing technology, 187-188: 637-630.
7. Khan Z.A., Lee B.H., Abdullah J(2005) Optimization of rapid prototyping parameters for production of flexible ABS object, Journal of materials processing technology 169 :54–61
8. Wang Tian Ming, Xi Jun Tong, Jin Ye (2007), A model research for prototype warp deformation in the FDM process, International journal of advance manufacturing technology, 33(11-12):1087-1096

9. Bellehumeur C.T., Gu P., Sun Q., Rizvi G.M. (2008). Effect of processing conditions on the bonding quality of FDM polymer filaments, Rapid prototyping journal, 14 (2): 72-80

10. Chou K, Y Zhang (2008), A parametric study of part distortion in fused deposition modeling using three dimensional element analysis, Proc. IMechE: Journal of engineering manufacture, 222(B):959-967.

11. R.Anitha, S.Arunachalam, P.Radhakrishnan(2001).Critical parameter influencing the quality of prototypes in fused deposition modelling, Journal of material processing technology, 118, 385-388.

12. Sanat Agrawal;S.G.Dhande(2007).Analysis of mechanical error in fused deposition process using a stochastic approach, International journal of production research.Vol.45, No.17,1 September 2007, 3991-4012.

13. P.M.Pandey, K.thrimurthulu,N.Venkata Reddy(2004). Optimal part deposition orientation in FDM by using a multicriteria genetic algorithm, International journal of production research.Vol. 42, No. 19, 4069-4089.

14. Stephen W.Tsai and Edward M. Wu.A (1970). General theory of strength for anisotropic materials, A journal of composire materials.

15. Stratasys (2004),FDM Vantage user guide version 1.1, www.stratasys.com.

16. Kathleen M. Carley, Natalia Y. Kamneva, Jeff Reminga (2004). Response surface methodology, CASOS Technical report.

17. Jae-Seob Kwak (2005). Application of taguchi and response surface methodologies for geometric error in surface grinding process, International journal of machine tools and manufacturing 45(2005) 327-334.

18. Pilipović Ana , Raos Pero and Šercer Mladen (2009), Experimental analysis of properties of materials for rapid prototyping, International journal of advanced manufacturing technology, 40: 105-115

19. Levy Gideon N., Schindel Ralf, Kruth J.P., Leuven K.U. (2003). Rapid manufacturing and rapid tooling with layer manufacturing(LM) technologies-State of the art and future perspectives, CIRP annals-Manufacturing technology, 52(2): 589-609

20. Chockalingama K., Jawahara N., Chandrasekarb U., Ramanathana K.N. (2008). Establishment of process model for part strength in stereolithography, Journal of materials processing technology, DOI 10.1016/j.jmatprotec.2007.12.144

21. Hopkinson N., Hagur R.J.M., Dickens P.H. (2006). Rapid manufacturing: An industrial revolution for the digital age, John Wiley & Sons, Ltd., England

22. Zhou M.Y., Xi J.T., Yan J.Q. (2004). Modeling and processing of functionally graded materials for rapid prototyping, Journal of materials processing technology, 146: 396-402

23. Bernarand Alain and Fischer A (2002). New trends in rapid product development, CIRP annals-Manufacturing technology, 51(2): 635-652

24. Pandey Pulak M., Jain Prashant K., Rao P. V. M.(2008), "Effect of delay time on part strength in selective laser Sintering", International journal of advance manufacturing technology, DOI 10.1007/s00170-008-1682-3

25. Vasudevarao Bharath, Natarajan Dharma Prakash, Razdan Anshuman, Mark Henderson(2000).Sensitivity of RP surface finish to process parameter variation, Solid free form fabrication proceedings, The University of Texas, Austin: 252-258

26. Sameh S. Habib (2009). Study of the parameters in electric discharge machining through response surface methodology approach, Journal of applied mathematical modelling.

27. Montgomery Douglas C. Design and analysis of experiments, 5th edition, John Wiley & sons (ASIA) Pte Ltd., Singapore

28. Noorani Rafiq (2006). Rapid prototyping: Principles and application, John Wiley & Sons, Inc. U.S.A.

29. Ken Jones, Mark Johnson, J.J. Liou (2006). The comparison of response surface and taguchi methods for multiple response optimization using simulation.

30. Che Chung wang, Ta-Wei Lin, Shr-Shiung Hu (2007) . Optimization of rapid prototyping process by integrating Taguchi method with grey relational analysis, Journal of rapid prototyping.Volume 13.Page 304-314.

31. Y. Ravi Kumar, C.S.P. Rao, T.A. Janardhan Reddy (2008). Robust process optimisation for fused deposition modelling, International journal of manufacturing technology and management 2008 - Vol. 14, No.1/2 pp. 228 - 245